ICTELS

International Conference on Technology, Engineering, and Life Sciences

16 - 19 May 2025
Rome, Italy

www.istes.org/event/ictels

Proceedings of International Conference on Technology, Engineering, and Life Sciences

Volume: 2

Editors

Assoc. Prof. Dr. Omid Noroozi, Wageningen University and Research, the Netherlands

Erdinc Cakir, Necmettin Erbakan University, Turkiye

Sabri Turgut, Necmettin Erbakan University, Turkiye

CONFERENCE PRESIDENTS

Dr. Mack SHELLEY - Iowa State University, United States

Dr. Wilfried ADMIRAAL - Leiden University, the Netherlands

Dr. I-Tsun CHIANG - National Taiwan Normal University, Taiwan

Dr. Wenxia WU - George Washington University, United States

SCIENTIFIC BOARD

Allan TARP - MATHeCADEMY, Denmark

Altay FIRAT - European University of Lefke, Cyprus

Andrea DEBELJUH - University Juraj Dobrila of Pula, Croatia

Brahim FERDI - Bechar University, Algeria

Branislav POPOVIĆ - University of Kragujevac, Serbia

Chalavadi SULOCHANA - Gulbarga University, India

Dariga NURKESHEVA - Nazarbayev University, Kazakhstan

Elizabeth ADAMSON - Edinburgh Napier University, United Kingdom

Farhad BALASH - Kharazmi University, Iran

Farouq ALMEQDADI - Emirates College for Advanced Education (ECAE), U.A.E.

Gordana SAVIC - University of Belgrade, Serbia

Haydar YUKSEK - Kafkas University, Turkey

Henry David KATNIYON - Federal College of Education, Pankshin, Plateau state, Nigeria

Hsin-Chih WU - National Taiwan Normal University, Taiwan

Janet VALDEZ - La Consolacion University Philippines, Philippines

Jessie BUSTILLOS - London Metropolitan University, United Kingdom

Kartika YULIANTI - Bina Nusantara University, Indonesia

Mesut AYDIN - Inonu University, Turkey

Milica PAVKOV HRVOJEVIĆ - University of Novi Sad, Serbia

Mohammad SARWAR - Scialert, Dubai, United Arab Emirates

Morteza BARIN - Farhangiyan University of Iran, Iran

Muteb ALQAHTANI - Rutgers University, United States

Nurten SARGIN - Necmettin Erbakan University, Turkey

Ognyan B. MANOLOV - European Polytechnic University, Bulgaria

Sanaa AL-DELAIMY - Mosul University, Iraq

Shynar BAIMAGANBETOVA - Nazarbayev University, Kazakhstan

Summer MOUALLEM - University of Central Lancashire, United Kingdom

Tamer USTUNER - Kahramanmaras Sutcu Imam University, Turkey

Tri Marhaeni PUDJI ASTUTI - Semarang State University, Indonesia

Yi-Teng HSU - National Taiwan Normal University, Taiwan

ORGANIZING COMMITTEE

Aliya MUSTAFINA - Nazarbayev University, Kazakhstan

Ann D. THOMPSON - Iowa State University, United States

Abdullatif KABAN - Ataturk University, Turkiye

Halil SNOPCE - South East European University, Macedonia

Hakan AKCAY - Yildiz Technical University, Turkey

Jacqueline T. MCDONNOUGH - Virginia Commonwealth University, United States

Mariusz JAWORSKI - Medical University of Warsaw, Poland

Mary M. CAPRARO - Texas A&M University, United States

Muhammad ZAYYAD - Al-Qasemi Academic College of Education, Israel

Murat BEYTUR - Kafkas University, Turkey

Mustafa PEHLIVAN - Necmettin Erbakan University, Turkey

Natela DOGHONADZE - International Black Sea University, Georgia

Natalija ACESKA - Ministry of Education and Science, Macedonia

Ossi AUTIO - University of Helsinki, Finland

O. Tayfur OZTURK - Necmettin Erbakan University, Turkey

Silvia MORARU - National High School Bucharest, Romania

Silviya KOSTOVA - The D.A. Tsenov Academy of Economics, Bulgaria

PARTICIPATING COUNTRIES

Türkiye	United States of America (USA)	Oman
Colombia	Indonesia	Lithuania
Sweden	Jordan	Romania
Morocco	Estonia	France
United Kingdom		

INDEXES

The publications affiliated with ISTES Organization are indexed or listed by all or some of the following sources:

SUPPORTED BY

ISTES EVENTS

International Conference on Research in Education and Science
06 - 10 May 2026 - Cappadocia, Nevsehir / Turkiye

International Conference on Education in Mathematics, Science and Technology
06 - 10 May 2026 - Cappadocia, Nevsehir / Turkiye

International Conference on Humanities, Education, and Social Sciences
15 - 18 May 2026 - Paris, France

International Conference on Technology, Engineering, and Life Sciences
15 - 18 May 2026 - Paris, France

International Conference on Humanities, Social and Education Sciences
09 - 12 April 2026 - New York, USA

International Conference on Life Sciences, Engineering and Technology
09 - 12 April 2026 - New York, USA

International Conference on Engineering, Science and Technology
15 - 18 October 2026 - Las Vegas, USA

International Conference on Social and Education Sciences
15 - 18 October 2026 - Las Vegas, USA

International Conference on Studies in Education and Social Sciences
05 - 09 November 2026 - Istanbul, Turkey

International Conference on Studies in Engineering, Science, and Technology
05 - 09 November 2026 - Istanbul, Turkey

BOOKS

SonSES

Studies on Social and Education Sciences

SonEST

Studies on Education, Science, and Technology

JOURNALS

IJEMST

International Journal of Education in Mathematics, Science and Technology

IJRES

International Journal of Research in Education and Science

IJonSES

International Journal on Social and Education Sciences

IJTE

International Journal of Technology in Education

IJTES

International Journal of Technology in Education and Science

IJonSE

International Journal on Studies in Education

IJSES

International Journal of Studies in Education and Science

IJonEST

International Journal on Engineering, Science and Technology

IJofES

International Journal of Education Science

IJofTES

International journal of Technology in Education Science

Table of Contents

From Data to Action: Leveraging E-learning Logs for Educational Decision-Making

Olga Ovtšarenko

TTK University of Applied Sciences, Estonia, Vilnius Gediminas Technical University, Lithuania,

(iD) https://orcid.org/0000-0003-3195-4280

Abstract: E-learning platforms generate vast amounts of log data that capture detailed records of learner interactions, providing a rich resource for understanding and improving the learning experience. This article explores how e-learning log data can be transformed into actionable insights to inform educational decisions. By examining key metrics and parameters in available streaming data, educators can identify areas for curriculum improvement, intervention strategies, and personalized learning paths. Data quality issues, privacy concerns, and the need for advanced analytics tools such as machine learning and data visualization techniques to harness the full potential of log data are discussed. The article analyzes case study from Estonian higher education institutions using log data from the Moodle platform to analyze learning outcomes and identify intervention strategies to prevent dropout/improve learning outcomes. The aim of this article is to provide actionable solutions for education stakeholders seeking to bridge the gap between raw data and actionable strategies by promoting a data-driven approach to e-learning optimization.

Keywords: E-Learning, Log Data, Optimization, Machine Learning

Introduction

The challenges of today's education system stem from the need to meet the diverse learning needs of students using rapidly evolving technological advances, which requires a personalized approach to align educational content with each student's knowledge portfolio and learning progress. The abundance of online information adds to another layer of complexity, making it difficult for students and educators to find and use relevant, high-quality content that meets educational goals.

The development of online recommendation systems has become essential to address these challenges. Such systems help users select and use the most appropriate e-learning resources to improve their knowledge and skills. However, traditional e-learning platforms use static content delivery methods that do not consider individual differences in learning styles, pace, or preferences. This lack of personalization results in decreased

engagement, suboptimal learning outcomes, and overall ineffectiveness of the educational process. However, the vast amount of data generated by student interactions in the digital environment remains largely untapped without effective methods for collecting, processing, and analyzing it to improve the learning process.

Affordable high-speed internet, data-driven technologies, and the ability to collect and process large data sets are being used across industries today, including education. Machine learning (ML), a branch of artificial intelligence, plays a vital role in using raw user activity log data to solve various problems. Using ML algorithms, it is possible to analyze complex data sets, identify patterns, and create personalized learning paths that meet students' individual needs. Not only do these systems dynamically adapt to student progress, but they also allow educators to optimize course structures and content delivery to improve outcomes.

E-learning platforms, especially in the wake of the COVID-19 pandemic, require adaptive learning technologies. Data stores have grown exponentially with the influx of information and advances in computational algorithms. However, this abundance of information can be overwhelming and difficult for learners to navigate effectively. Adaptive learning systems that use machine learning algorithms can track learners' progress, analyze interactions, and prevent information overload.

This study uses machine learning algorithms to process e-learning log data to optimize learning and prevent learner dropout. Objectives include:

- Collect detailed student interaction data from e-learning platforms.
- Develop pre-processing methods to clean and structure data for ML models.
- Use ML algorithms to identify critical learner characteristics to create personalized adaptive learning paths.

With this approach, educators can harness the power of data to enhance learning experiences, improve learning outcomes, and create an adaptive e-learning framework.

The paper is organized as follows: Section 2 gives an overview and analysis of existing e-learning adaptation methods and methods of automating the learning path. Section 3 explains the methodology and the concept of a model of adaptive e-learning material for a student's independent work. Section 4 presents the Results of a general conceptual framework for intelligent adaptive learning systems and their components. Section 5 presents a Discussion of the Results, and Section 6 contains concluding remarks.

Related Works

Continuous technological advancement has replaced traditional learning schemes with modern eLearning solutions, which offer more flexibility and freedom for students to learn at their own pace and time using computers, mobile devices, tablets, and internet facilities. Unless a proper scientific study is conducted to determine the effect of specific barriers in implementing an eLearning system, developing a high-tech eLearning system is not enough (Solangi et al., 2018).

E-learning Affecting Factors marked in (Mahdavi Ardestani et al., 2023; Mohammed et al., 2024) include factors that influence the effectiveness of e-learning:

• Learner factors - characteristics, self-regulation and engagement.

Behavioral intentions and habits according to (Zheng et al., 2025), or habitual behavior, significantly influence students' intentions to engage with e-learning platforms.

Research (Abdullah et al., 2024) shows that students' ability to self-regulate their learning processes directly impacts their engagement and experience in the online learning environment. Effective self-regulation is correlated with higher satisfaction and better academic performance.

• E-course factors - structure and design.

Developing e-course guides: Clarity of goals and objectives, organization of materials and use of interactive learning objects significantly influence student perception, ensuring their interest and engagement (Walt et al., 2024). Description and explanation of e-course results - certification and acquisition of skills, increases its attractiveness. Providing feedback from the teacher through automated comments on results, live sessions, forums improve the learning process (Safitri et al., 2022).

An analysis of e-learning trends shows the growing importance of personalized learning (Bashir & Lapshun, 2024), the integration of artificial intelligence into learning, and the development of hybrid e-courses that combine online and face-to-face learning.

Flexibility and accessibility - the ability to choose learning schedules and access resources on-demand accommodates the diverse needs of learners. Content should be accessible to learners with different needs, including those with disabilities, through options such as closed captioning, transcripts, and adaptive technology.

• Factors that Ensure Academic Success.

Student Satisfaction: Factors that influence satisfaction with online learning include the quality of interaction with instructors, availability of support services, and clarity of course content (Yu, 2022). The positive impact of these factors ensures student satisfaction.

Academic Success: The impact of online learning on student achievement is supported by well-structured online courses, if students are supported by interactivity of resources, automated assessment, and recommendations (Akpen et al., 2024).

• Technological Support.

Usability of the platform with intuitive navigation and a user-friendly interface greatly facilitates learning without creating obstacles and wasting time.

Device compatibility ensures uninterrupted learning of e-course content when changing gadgets and is of great importance to students (Oyetade et al., 2023). A stable internet connection and sufficient speed are a prerequisite for continuous learning, especially for media-intensive courses.

Understanding learner characteristics, technology and content design elements, external influences and their interactions is essential for developing effective e-learning strategies to improve student satisfaction and academic performance. The multifaceted nature of factors influencing e-learning makes it possible to use different combinations of them to measure the impact on learning success.

Measuring the impact of various factors on e-learning effectiveness is critical to optimizing learning outcomes. Analyzing learner interactions with online learning modules provides insight into learner engagement and the effectiveness of learning resources. Metrics used to assess learning outcomes included time spent using learning resources, frequency of access, and assessment effectiveness (Leitão et al., 2020). Using data analytics to monitor and predict learning behavior has proven to be effective. By analyzing patterns in student data, educators can determine which factors have the most significant impact on learning outcomes. The study (Chen and Guthrie, 2019) examined the effectiveness of learning resources by analyzing learners' interactions with online modules, providing actionable insights for course improvement.

The suitability of an eLearning pathway is determined by the complex interaction of learner characteristics, content quality, technology infrastructure, and contextual factors. Tailoring eLearning experiences to address these variables can lead to more effective and inclusive education, benefiting learners from different demographics. As technology evolves, continuous adaptation and refinement of eLearning strategies will remain vital to promoting successful educational outcomes.

According to Hou & Fidopiastis (2016), the goals of adaptive learning systems are:

• tracking the learning style and progress of students,

• monitoring the physical and emotional state of the student,

• monitoring the appropriate state of the learning environment,

• monitoring the impact of recommendations on the student,

• monitoring student feedback and its impact on the learning environment,

• setting up interaction management.

These goals must be considered when designing educational material and planning for its adaptability. When developing the structure of educational material, it is essential to consider what skills, knowledge and competencies a student should receive and correctly determine the order and connection of the topics of the entire course.

Method

This study focuses on evaluating and analyzing the performance of different tools used in an educational environment for e-course data model use for predictive analysis. The methodology includes calculating parameter weights that affect the performance of a tool, including tool weight, ECTS weight, and log weight.

Creation of An E-Course Data Model Based on Historical Student Activity Log Records

The study used and processed historical data from Tallinn University of Technology, Estonia, activity logs of 37 students studying the e-course "Construction Investments and Project Management", 9 ECTS, from February to

May 2024, and the e-course structure developed by e-course creator (see Figure 1). The levels of arrangement of educational resources by topic correspond to the levels of complexity of Bloom's taxonomy and are marked with different colors.
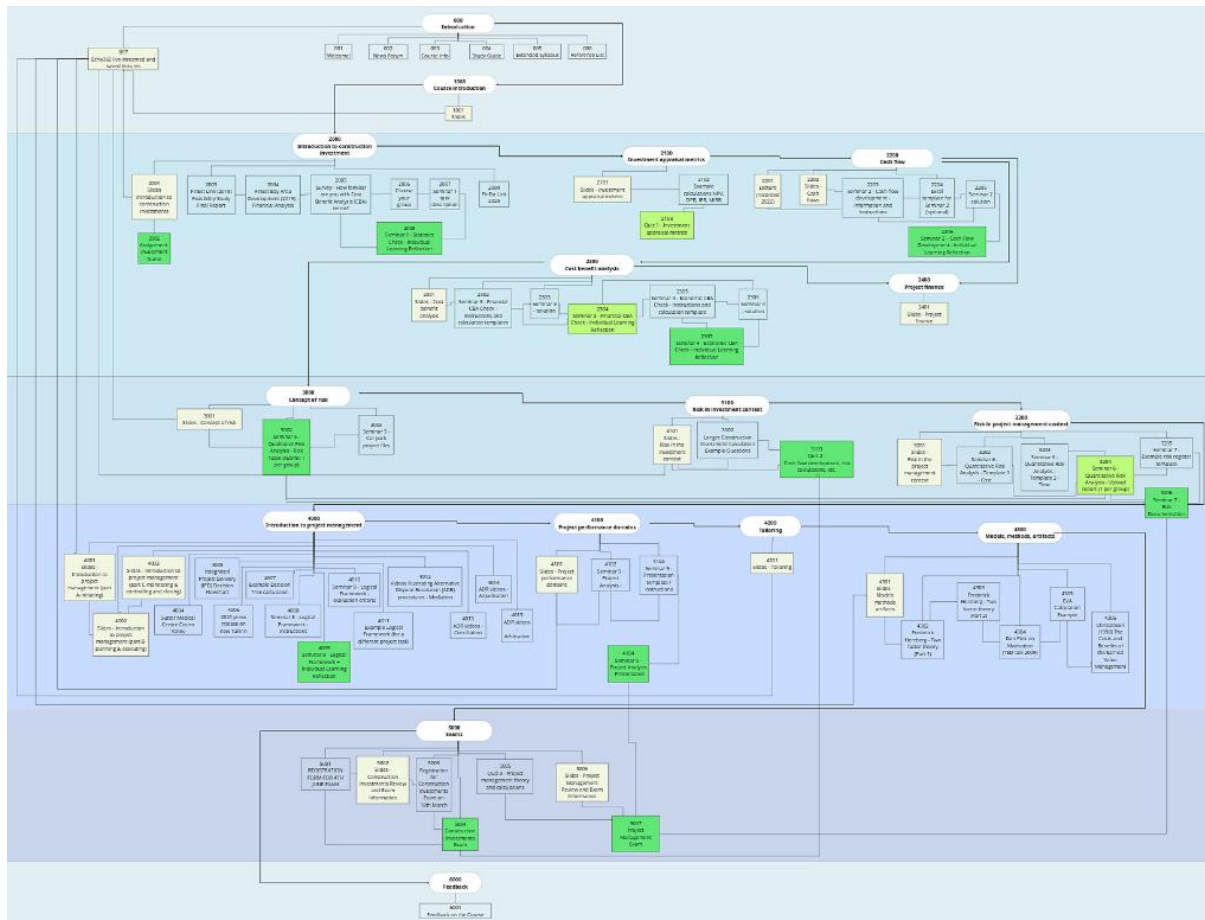
Figure 1. E-Course Taxonomy (Ovtsarenko, 2025: Collection_3, E-Course Taxonomy).

Data Collection and Preprocessing

Processing a large amount of data (78,000 rows of records, and after cleaning the log data, the work continued with 39,000 records), additional weighted parameters were aggregated to calculate the performance of each e-course resource and improve the model in preparation for predictive analysis. The dataset (Ovtsarenko, 2025: Collection_3, E-course dataset) consists of several tools with associated attributes, such as:

- tool_performance calculated indicator of the effectiveness of e-course resources (see Equation 1),
- tool_code: a unique identifier for each tool, appointed by teacher,
- tool_weight: a measure of the relative importance of the tool (see Equation 2),
- ECTS_weight: the assigned weight is based on the European Credit Transfer and Accumulation System (ECTS) (see Equation 3),

• log_weight: log weight - the interaction of the student's use of the e-course resource,

• level_index: a numeric representation of the hierarchical level of the tool in the curriculum.

Missing values in the dataset were handled using median imputation for numeric attributes and default string values for categorical attributes. In Table 1 are presented data for model use in Colab Notebook. In Table 1 the calculated data of fifty e-course resources are presented.

Table 1. E-Course Dataset

	tool_code	tool	activity	level	level_index	tool_weight	tool_ECTS	logs	log_weight
1	001	1	Welcome!	1_basic info	2	0.009852	2.328358	54	0.00140
2	002	1	News Forum	0_adm	1	0.004926	1.164179	230	0.00596
…	…	…	…	…	…	…	…	…	…
18	2007	1	Seminar 1 task description/ Wiki: FinEst Link 2024	2_applied	3	0.014778	3.492537	967	0.02507
19	2008	1	Seminar 1 - Statistics Check - Individual Learning Reflection	3_reflective	4	0.019704	4.656716	721	0.01869
20	2009	1	FinEst Link 2025	2_applied	3	0.014778	3.492537	11	0.00028
…	…	…	…	…	…	…	…	…	…
39	2307	1	Seminar 4 - Economic CBA Check - Individual Learning Reflection	3_reflective	4	0.019704	4.656714	605	
	…	…	…	…	…	…	…	…	…

In addition, the Excel file sheets (Ovtsarenko, 2025: Collection_3, E-course dataset) contain codes of students who have completed the e-course, as well as cleaned and prepared data for building a data model.

Calculating Weighted Parameters

To calculate the tool (e-course resourse) performance (see Equation 1), a refined formula was introduced to balance the influence of different parameters (Ovtsarenko, 2025: Collection_3, E-course dataset):

$$P^{Tool} = W^{Tool} * W^{ECTS}/ W^{Log},\qquad(1)$$

where

P^{Tool} - tool_performance, representing the efficiency of the course resources used

W^{Tool} - tool weight, represents the weight assigned to the tool based on its importance in the learning process, calculated by Equation (2)

$$W^{Tool}= \text{(tool's level\_index determined by the teacher from 1 to 5)/ (total value of levels)},\qquad(2)$$
$$\text{whereas } \Sigma W^{Tool} = 1$$

W^{ETCS} - ECTS weight for each course resource, represents the teacher's planned time in hours (see Equation 3)

$$W^{ETCS} = W^{Tool} * \Sigma\ W^{ECTS},\qquad(3)$$
$$\text{whereas } \Sigma W^{ECTS} = 9(ECTS) * 26\ (hours)$$

W^{Log} - log_weight, representing the actual use of each resource considering student activity.

The developed course model was used with machine learning algorithms to verify the obtained results (Ovtsarenko, 2025: Collection_3, EPX Weighted parameters calculation visualization).

Weighted Parameters Correlation Matrices

The correlation matrix (see Figure 2) demonstrates how strongly different tool parameters are related to each other. The values range from -1 (negative correlation shown in blue color that means one increases, the other decreases) to 1 (positive correlation in red color and meaning variables increase/decrease together):

- tool_weight vs tool_ECTS (1.00) - these are perfectly correlated, meaning they likely contain the same or proportional values. This suggests redundancy in the dataset, meaning one might be removed to simplify the model and suggesting that the formula may need adjustments to introduce more independence in performance evaluation,
- tool_weight vs tool_log (0.96) – a very strong correlation, but not perfect,
- tool_weight vs tool_performance (0.99) - tool performance is heavily dependent on tool_weight, which makes sense because the formula includes tool_weight. The high correlation means tool_weight plays a dominant role in determining performance,

- tool_ECTS vs tool_performance (0.99) - a very strong correlation, suggesting that ECTS weight is almost directly proportional to performance,

- tool_log vs tool_performance (0.96) - while still highly correlated, tool_log has slightly less impact on performance compared to tool_weight or tool_ECTS. This makes sense since tool_log is a transformation meant for normalization, and its effect is slightly scaled down. tool_log plays a normalizing role but remains strongly correlated with other metrics, meaning it smooths values without drastically altering relationships.
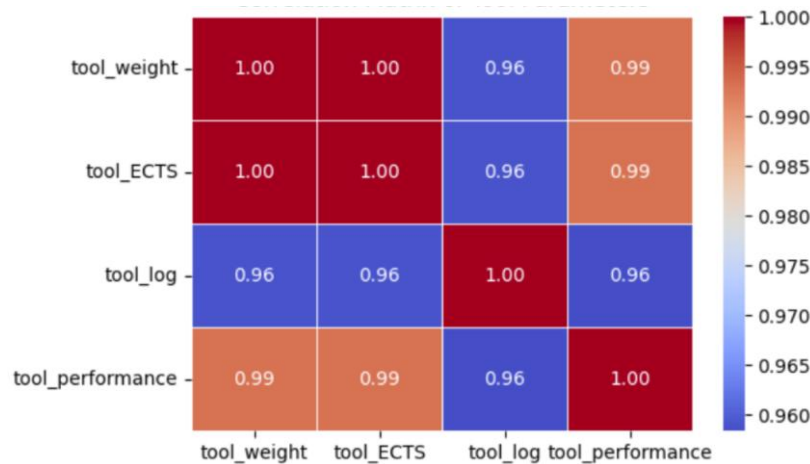
Figure 2. Correlation Matrix of Tools' Parameters (Ovtsarenko, 2025: Collection_3, Tool Performance).

Validity Analysis

The ML algorithm was used to check the reliability and efficiency of the obtained data:

- Pearson Correlation (Wt_ECTS vs. Log Weight) = 0.987.

  Pearson Correlation measures the linear relationship between Wt_ECTS (the calculated weight) and log_weight (the weight of the student's resource usage). A value of 0.987 indicates a strong positive linear correlation, meaning log_weight is very closely related to Wt_ECTS with virtually no deviations.

- Spearman Correlation (Wt_ECTS vs. Log Weight) = 1.000.

  Spearman Correlation measures a monotonic relationship (whether higher values in one column correspond to higher values in the other, regardless of linearity). A value of 1.000 means a perfect rank correlation, meaning Wt_ECTS and log_weight always increase together in the same order.

This means that the e-course model is valid and works correctly.

Improving the student data model for prediction

The parameters are normalized and scaled to improve the student data model and obtain more reliable results (Ahsan et al., 2021), and the model performance varies depending on the data scaling method. Empirically selected coefficients (Hyndman & Athanasopoulos, 2018):

- alpha_fitted = 0.7, this might give more weight to recent learning activities or tool use.
- beta_fitted = 0.3 (the typical default range is 0.1 to 0.4). This parameter controls how much weight is given to changes in trend over time and useful for modeling student progress or course difficulty over time.
- gamma_fitted = 0.1 (Typically ranges from 0.05 to 0.3). It affects how well the model adapts to recurring patterns of learning.

As a result of using the machine learning algorithm, the most suitable coefficients for scaling the parameters were selected, which made it possible to improve and optimize the data model.

The correlation of the data model parameters has also changed and has become smoother as shown in Figure 3.

The values of the coefficients were not significantly changed, which confirms the model's functionality.

```
--- Fitted Parameters ---
Alpha (tool_weight): 1.0516
Beta (ECTS_weight): 0.7738
Gamma (log weight shift): -0.0079

Pearson Correlation (Wt_ECTS vs Log Weight): 0.985
Spearman Correlation (Wt_ECTS vs Log Weight): 1.000
```
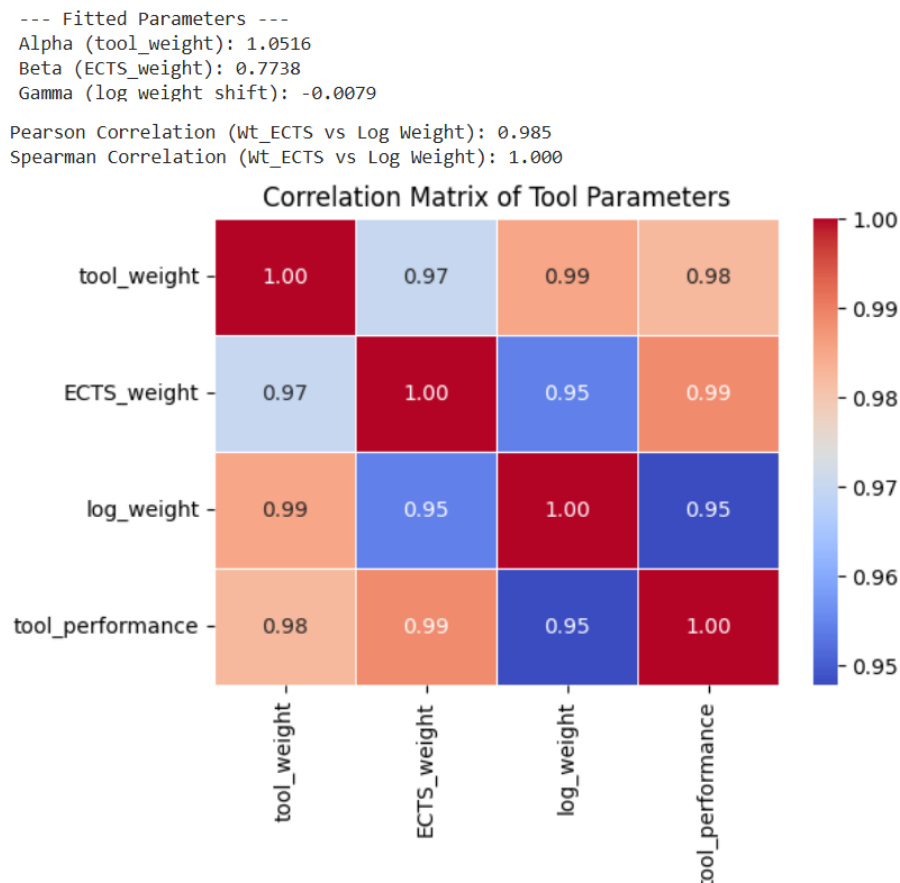

Figure 3. Updated Normalization Coefficients and Correlation Matrix of Tools' Parameters (Ovtsarenko, 2025: Collection_3, Tool performance Predicted).

E-course Structure Visualization

To understand the relationship between educational resources within this course, considering their content and

complexity, was built a visual 3-dimensional structure of the e-course (see Figure 4). The values 'Tool Code' were used along the X axis, 'ECTS Weight' along the Y axis, and 'Log Weight' along the Z axis.

The resulting diagram demonstrates the dependence of resources on their level of complexity and the relationship of resources to each other, which allows the course developer to optimize the course structure for more successful use of educational resources by students.

This visualization is also very informative for students who can independently plan how to use educational resources to achieve the desired result.

Figure 4. 3D Visualization of Tool Weights with Connections.

Python Blocks Resources Used for Study

The study used four libraries described in Table 1, Python's primary tools for data processing and analysis workflows.

Table 1. Import Block in Python Data Analysis Scripts

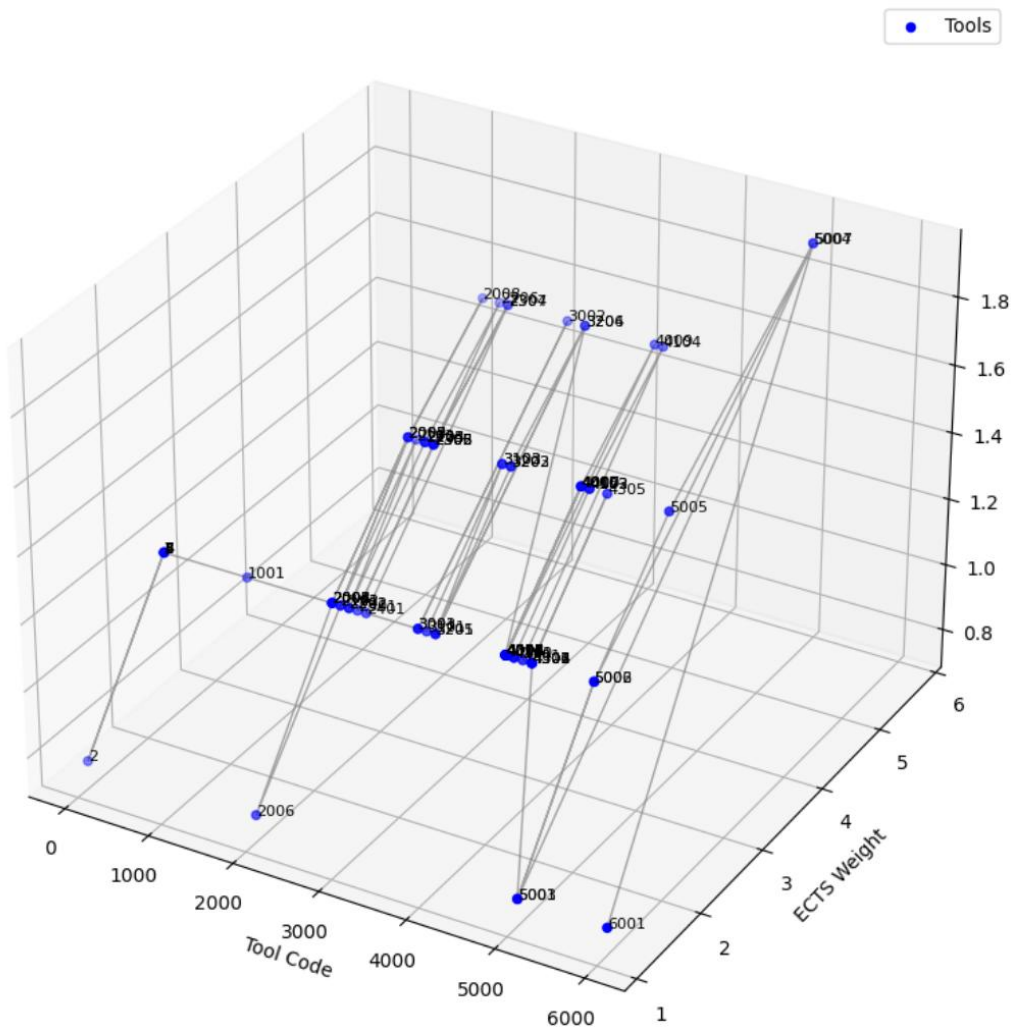| Library	Alias	Purpose
pandas	pd	DataFrames, reading/writing tabular data
numpy	np	Numerical operations, arrays, math functions
matplotlib.pyplot	plt	Basic plotting (line, scatter, bar)
seaborn	sns	Enhanced plotting (statistical + aesthetic)

Pandas' library import is used to handle structured data such as tables to read and write Excel/CSV files, manage columns, filter rows, merge data, etc. (McKinney, 2010).

NumPy, a library for numerical computing, is used for mathematical operations on arrays and numeric data, generating random numbers, and linear algebra (Harris et al., 2020).

Matplotlib is a plotting module that creates visualizations such as line plots, bar charts, histograms, and scatter plots (Hunter, 2007).

Seaborn is a statistical data visualization library built on Matplotlib. It creates more attractive and informative visualizations with less code and adds built-in support for box plots, heatmaps, regression plots, and more (Waskom, 2021).

Results

The proposed method for developing and using an e-course model to facilitate adaptive and effective learning includes several stages. To enable automation of a specific stage using ML algorithms, each stage of e-course development and use is analyzed. The approach to e-course development, as well as the corresponding success indicators and the possibility of automating a specific stage are outlined in Table 2.

Table 2. Adaptive E-Course Structure

Stage	Conditions	Data of successful metrics	Action
1	registration/ fill out the user profile	results/ratings/ time spent on training	automation
2	pre-test/ assessment of prior knowledge	results/ratings/ time spent on training	automation
3	the sequence of studying topics	the number of user connections/ time spent on training	automation
4	current testing	results/ratings/ time spent on training	automation

	International Conference on Technology, Engineering, and Life Sciences	
ICTELS		iSTeS
www.ictels.net	May 16-19, 2025 Rome, Italy	www.istes.org

5	virtual tutor recommendations for student mastering /progress evaluation	expert opinion	semi-automation
6	post-testing	results/ratings/ time spent on training	automation
7	feedback from the tutor/virtual tutor with recommendations for the next stage of learning	virtual tutor expert opinion/suggestions	automation/ reflections text
8	feedback from students for the teaching quality index	student opinion/ satisfaction	reflections text

The metrics presented in the table demonstrate that expert control and participation are also necessary in addition to the use of machine learning methods.

Discussion

Proposed for discussion possibilities of using this method for predictive analytics and forecasting student learning:

- Predicting student performance based on learning weights.

Weighted parameters (log_weight, tool_weight, etc.) can be used to predict how much effort a student needs to put in to succeed. If a tool has a high tool_ECTS, students may need more time to study or better preparation to succeed. The model can help identify courses/tools with high effort and suggest customized study plans.

- Optimizing course and curriculum design.

By analyzing correlations between tool_weight, tool_ECTS, and student performance data, the model can highlight which tools contribute most to student success. If tool_log shows that some tools have low engagement but high weight, they may need to be redesigned. Course designers can optimize course structures to make learning more efficient.

- Student Performance Prediction and Early Intervention.

The model can be combined with historical student performance data (grades, engagement metrics).

If a student is struggling with high-weight tools (tool_ECTS), the system can issue an early warning and suggest interventions (tutoring, additional materials) to reduce dropout rates and improve student performance.

- Personalized Learning Paths.

By clustering students based on their engagement across tools, it is possible to create customized learning paths: a fast learner will master advanced modules faster. A struggling learner will receive more basic resources before moving up. This creates an adaptive learning experience, improving retention and comprehension.

- AI-powered Student Recommendations.

Using machine learning, the model can suggest recommended learning paths based on the success patterns of previous students. If students with a similar profile have succeeded using a certain set of tools, new students

can be recommended the same approach.

The proposed structure and recommendations can help in teaching various subjects. To achieve this, using the reference model of educational material structure will require introducing new data and possible adjustments, in line with the competencies of this subject and focusing on the specific needs of users.

The use of various criteria to create a dynamic adaptive learning environment that tailors a learner's learning path is appropriate and very promising, as it maximizes the use of the most relevant learning methods for different stages in the study of e-course topics. AI is effective for automated metadata collection and processing. However, other methods of collecting and processing information should be included with the participation of learning environmental administrators and creators of educational material.

For future research, the author plans to identify the most effective methods for collecting and processing learning analytics information at each stage of model usage and conduct experiments with students in technical specialties to test the proposed model.

Conclusion

In the study of student activity in studying an e-course, the weighted parameters method was used to aggregate additional parameters and create a data model, the purpose of which is to analyze learning outcomes and determine intervention strategies to prevent dropout/improve learning outcomes.

Validation of the data model with aggregated parameters showed its performance for predictive analytics. Using this data model in ML algorithms in combination with the obtained historical data of student results can be used to predict learning outcomes, prevent student dropout and generate recommendations depending on the student's acquired knowledge to improve his/her learning.

Also, the method used is very useful for course developers to clarify and improve the structure of the e-course, understand the effectiveness of using educational resources and develop additional useful resources / clarify the content of existing ones. Proper content sequence is crucial for facilitating effective learning by ensuring that students' progress through the material logically and coherently, thereby maximizing comprehension and retention (OECD, 2025). By using strategic sequencing techniques, instructional designers create a planned learning path that supports students' cognitive processes and improves overall learning outcomes:

- Analyzing learning objectives helps determine the logical order in which content is presented.
- Organizing content into manageable chunks with a clear focus builds on previous material, utilizing headings, subheadings, and visual cues for better orientation.
- Assessing students' prior knowledge helps identify prerequisite concepts that students must master before

progressing to more complex topics. This way, prerequisite knowledge is gradually built upon, providing a solid foundation for understanding advanced concepts.

- Concepts progress from simple to complex, allowing for a gradual difficulty curve that enables students to absorb and integrate knowledge effectively.

- A patterned learning experience provides appropriate support and guidance throughout the learning process, initially offering instructions and directions, with support gradually decreasing as students acquire skills. More challenging tasks can be introduced progressively as students demonstrate proficiency.

- Reinforcement and retrieval practice throughout the learning sequence improve long-term retention. Periodic review of previously covered material strengthens learning by enhancing neural connection.

- Engaging students with interactive activities at strategic points in the learning sequence allows them to apply knowledge and skills in real-world settings, promoting active learning and reinforcing understanding.

Adaptation of the learning environment using advanced machine learning methods as adaptive logic depending on the changing level of student knowledge is designed to provide a new level of modern personalized learning.

Acknowledgement

References

Ahsan, M. M., Mahmud, M. A., Saha, P. K., Gupta, K. D., & Siddique, Z. (2021). Effect of Data Scaling Methods on Machine Learning Algorithms and Model Performance. Technologies, 9(3), 52. https://doi.org/10.3390/technologies9030052.

Abdullah, M. N. L. Y., Saw Fen, T., Samsudin, M. A., Tze Ying, S., & Yuan, C. F. (2024). Factors influencing undergraduate students' online learning outcomes: A structural equation modeling. SAGE Open, 14(2).

Akpen, C. N., Asaolu, S., Atobatele, S., Okagbue, H., & Sampson, S. (2024). Impact of online learning on student's performance and engagement: A systematic review. Discover Education, 3, 205.

Bashir, S., & Lapshun, A. L. (2024). E-learning future trends in higher education in the 2020s and beyond. Cogent Education, 12(1).

Chen, Z., & Guthrie, M. (2019). Measuring the effectiveness of learning resources via student interaction with online learning modules. arXiv.

Harris, C. R., Millman, K. J., J., S., Gommers, R., Virtanen, P., Cournapeau, D., Wieser, E., Taylor, J., Berg, S., Smith, N. J., Kern, R., Picus, M., Hoyer, S., Van Kerkwijk, M. H., Brett, M., Haldane, A., Del Río, J. F., Wiebe, M., Peterson, P., . . . Oliphant, T. E. (2020). Array programming with NumPy. Nature, 585(7825), 357-362. https://doi.org/10.1038/s41586-020-2649-2.

Hou, M., & Fidopiastis, C. (2016). A generic framework of intelligent adaptive learning systems: From learning effectiveness to training transfer. Theoretical Issues in Ergonomics Science.

Hunter, J. D. (2007). Matplotlib: A 2D graphics environment. Computing in Science & Engineering, 9(3), 90–95. https://doi.org/10.1109/MCSE.2007.55.

Hyndman, R.J. & Athanasopoulos, G. (2018). Forecasting: Principles and Practice. https://otexts.com/fpp3/.

Leitão, G., Colonna, J., Monteiro, E., Oliveira, E., & Barreto, R. (2020). New metrics for learning evaluation in digital education platforms. arXiv.

Mahdavi Ardestani, S. F., Adibi, S., Golshan, A., & Sadeghian, P. (2023). Factors influencing the effectiveness of e-learning in healthcare: A fuzzy ANP study. Healthcare (Basel), 11(14), 2035.

McKinney, W. (2010). Data structures for statistical computing in Python. In S. van der Walt & J. Millman (Eds.), Proceedings of the 9th Python in Science Conference (pp. 51–56). https://doi.org/10.25080/Majora-92bf1922-00a.

Mohammed, A. B., Maqableh, M., Qasim, D., & AlJawazneh, F. (2024). Exploring the factors influencing academic learning performance using online learning systems. Heliyon, 10(11), e32584.

OECD (2025), Unlocking High-Quality Teaching, OECD Publishing, Paris, https://doi.org/10.1787/f5b82176-en.

Ovtsarenko, O. (2025, April 5). Collection_3. figshare. Retrieved from https://doi.org/10.6084/m9.figshare.c.7755035.v1.

Oyetade, K., Harmse, A., & Zuva, T. (2023). Factors influencing students' use of e-learning technologies. International Journal of Learning, Teaching and Educational Research, 22(9), 617–632.

Safitri, S., Setiadi, H., & Suryani, E. (2022). Educational data mining using cluster analysis methods and decision trees based on log mining. Jurnal RESTI (Rekayasa Sistem dan Teknologi Informasi), 6(3).

Solangi, Z. A., Al Shahrani, F., & Pandhiani, S. M. (2018). Factors affecting successful implementation of eLearning: Study of Colleges and Institutes Sector RCJ Saudi Arabia. International Journal of Emerging Technologies in Learning (iJET), 13(6), 223–230.

Van der Walt, F., Anele, N., & Mpho, T. (2024). The influence of selected factors on perceived enjoyment of the online learning experience: Lessons for post-COVID-19 classrooms. Frontiers in Education, 9.

Waskom, M. L. (2021). Seaborn: Statistical data visualization. Journal of Open Source Software, 6(60), 3021. https://doi.org/10.21105/joss.03021.

Yu, Q. (2022). Factors influencing online learning satisfaction. Frontiers in Psychology, 13.

Zheng, H., Han, F., Huang, Y., Wu, Y., & Wu, X. (2025). Factors influencing behavioral intention to use e-learning in higher education during the COVID-19 pandemic: A meta-analytic review based on the UTAUT2 model. Education and Information Technologies.

Data Mining Framework for Predicting Maintenance Services of Automobiles

Abbas Al-Refaie

Department of Industrial Engineering, University of Jordan, Amman, Jordan,

https://orcid.org/0000-0002-7845-5633

Abstract: This research develops a data mining framework for predicting Maintenance services (MS) for cars under warranty. Data on MS was obtained from a recorded database for 1080 cars with 980 spare part replacements recorded over six months. The generalized sequential patterns (GSPs), association rules, and rule-based classification were performed on the collected MS data and validated using test data. The significant frequent sequential patterns (FSPs) were then identified without car attributes. Similarly, the significant FSPs were determined considering car attributes; production year, engine type and capacity, and mileage for repair. Moreover, significant FSPs for spare part replacement were found. Finally, joint prediction of FSPs for MS and spare part usage was carried out. The results showed that the predicted MS is engine repair in the first month, tire repair in the second month, and spare part replacements of car engines in the fourth month. Further, the main car attributes in the next MS were engine capacity (CAP_2) of more than 1800 cc, cars with internal combustion (IC) and CAP_2 engines travelled more than 18,000 miles. In conclusion, the resulting significant FSPs support the development of effective planning of MS, enhancing customer satisfaction, and efficient control of spare part inventory.

Keywords: Data Mining, Automobile, Frequent Sequential Patterns, Warranty, Spare Parts

Citation: Al-Refaie, A. (2025). Data Mining Framework for Predicting Maintenance Services of Automobiles. In O. Noroozi, E. Cakir & S. Turgut (Eds.), *Proceedings of ICTELS 2025-- International Conference on Technology, Engineering, and Life Sciences* (pp. 16-32), Rome, Italy. ISTES.

Introduction

Worldwide the automobile market is the fastest-growing industry that drives economic growth (Hartung et al., 2020). Efficient maintenance services (MS) including repairing or replacing components are crucial in the market growth of the automobile industry (Al-Refaie & Aljundi, 2024; Al-Refaie & Al-Hawadi, 2023; Al-Refaie & Almowas, 2023; Al-Refaie et al., 2023). Thus, the spare parts should be available at the desired amount and time. However, information on failure occurrence time, type, and spare parts is typically uncertain (Jacobs et al., 2019). Therefore, for automobiles under warranty, prediction of frequent sequential patterns (FSPs) of MS with the required spare parts should be planned concurrently (Srinivasan et al., 2016).

	International Conference on Technology, Engineering, and Life Sciences	
ICTELS		iSTES
www.ictels.net	May 16-19, 2025 Rome, Italy	www.istes.org

The shift from product to service-based operation in the automotive industry has made predictive maintenance crucial to ensure customers with uptime guarantees (Al-Refaie & Al-Hawadi, 2022; Al-Refaie et al., 2022). In practice, the sudden failure of one component of a car can cause severe and costly subsequent failures of other components (Al-Refaie et al., 2020; Al-Refaie & Hanayneh, 2014). For example, the wear of gears can cause knocking in transmission. Ignoring information about component failure may increase the corrective maintenance costs of the next component repair or replacement. For cars under warranty, maintenance engineers face the challenge of predicting the sequence of MS with the necessary spare parts required for replacement. Consequently, identifying the sequence of MS and using spare parts has become the main objective in maintenance planning (Buddhakulsomsiri & Zakarian, 2009).

The sequential pattern (SP) mining technique is an effective technique for extracting the frequent sequence patterns (FSPs) of MS and predicting the required spare parts (Buddhakulsomsiri et al., 2006; Romanowski & Nagi, 2001). This technique searches relations or patterns among data objects based on information gathered in the maintenance database with timestamps (Bastos et al., 2014). It relies on testing various sequential patterns of MS and spare parts to determine the significant FSPs using several measures including support, confidence, coverage, and lift, and then use those FSPs to predict the MA and spare parts for future periods.

Data mining and utilization have various goals in the automotive industry including consumer behaviour, resource optimization, product development, production processes, and services (Simmachan et al., 2023; Llopis-Albert et al., 2021; Wang and Kim, 2020). The maintenance transaction records main information about car attributes such as engine type, engine capacity, mileage for repair, and production year. In addition, information about performed MS, component repair, or replacement, is also recorded (Bastos et al., 2012). Such information enables maintenance engineers to examine the relationship between the MS at the current period and plan actions for the next period's maintenance (Awwalu et al., 2014).

In addition, the predicted failure sequences of MS and spare parts can support effective control of spare parts inventories, determining warranty policy, and efficient utilization of maintenance resources, development, and management (Patel, 2021; Zabinski et al., 2021; Rasheed, 2014; Prytz et al., 2013). Therefore, this research develops a data-mining framework to predict the frequent sequential patterns of maintenance services for automobiles under warranty. The remaining of this research including the introduction is organized as follows. Section 2 reviews relevant studies on maintenance prediction for the automobile industry. Section 3 presents the application of the data-mining framework. Section 4 discusses the research results. Section 5 summarizes research conclusions, limitations, and future studies.

Literature Review

The data mining techniques have been widely applied to achieve distinct goals in the automobile industry. For example, Teo (2010) considered data mining and modeled the mean cumulative warranty cost or number

of claims (per vehicle) in automotive warranty analysis. Moharana & Sarmah (2015) determined the optimal kit for spare parts used in various equipment by association rule mining at minimum support and penalty costs. Moharana et al. (2019) used data mining to extract the SPs of MS and related spare parts utilizing information from historical maintenance records. Romelfanger and Kolich (2019) used big data analytics for automotive seat design practices related to thigh support and cushion length, a consistent customer complaint across the automotive seating industry in the North American market. Salmi & Atif (2021) detected fraudulent automobile insurance claims using a data mining approach, random forests, and logistic regression. Xu and Gui (2021) conducted a prediction of technology in new energy vehicles in China using data mining techniques. The frequent pattern growth algorithm and input-output analysis were used to construct a new technology prediction method. Chen et al. (2021) used a deep learning-based approach for automobile remaining useful life prediction models using a sizable real-world fleet maintenance dataset for a UK fleet company. Wakiru et al. (2021) developed a maintenance decision support system (DSS) framework using in-service lubricant data for fault diagnosis. Cheng et al. (2022) constructed an intelligent gear decision method and design methodology for a vehicle automatic transmission system by using a data mining method. Al-Refaie et al. (2023) adopted generalized sequential patterns and association rules in data mining to predict MS with and without attributes of washing machine products. Astuti & Yuniarti (2023) applied data mining with a k-means to data sales of automotive products in Indonesia. Al-Refaie & Hamdieh (2024) integrated sequential patterns and spare parts for predicting MS in the water-cooled chiller products under warranty. İfraz et al. (2024) employed the SP mining on gearbox failure data, and spare parts to predict MS and spare parts in a bus fleet.

This research contributes to the ongoing research on data mining applications in the automobile industry by predicting the FSPs of MS and necessary spare parts during the next periods for automobiles under warranty.

thod

The data mining techniques were applied to the collected data shown in Fig. 1 for 1080 cars under a warranty period of six months.
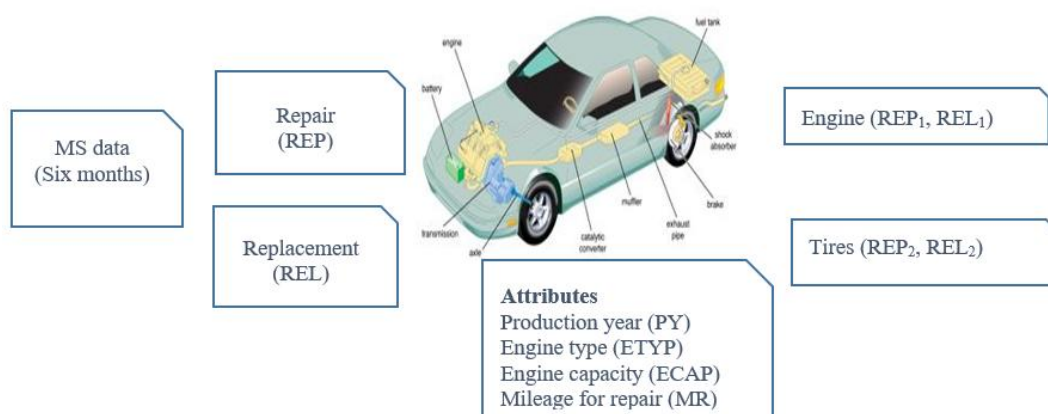

Figure. 1. Illustration of MS Data and Car Attributes.

The car attributes were Production year (PY) or car model {M_1: 2021, M_2: 2022}, Engine type (ETYP): {HD: Hybrid, IC: Internal combustion}, Engine capacity (ECAP, cc): {less than or equal 1800 ($ECAP_1$), more than 1800 ($ECAP_2$)}, and Mileage at repair (MR, Miles): {MR_1: less than or equal 18000 miles, MR_2: more than 18000 miles}. The data covered the monthly MS; repair (REP) or replacement (REL), for car engines and tires at various combinations of car attributes as shown in Table 1. The description of MS for the car's engine and tires is provided in Table 2. The number (S) of spare parts replacements for car engines and tires during 6 months without considering the time that occurred were 980 and 680 activities, respectively. Table 3 displays the spare parts used for the engine (S_{11}, S_{12}, S_{13}, and S_{14}) and tires (S_{21}, S_{22}, S_{23}). Tables 4 and 5 display the spare parts conducted in each replacement for car engines and tires, respectively, where 1 indicates that this spare part was replaced, and 0 otherwise.

Table 1. Collected Car MS Data.

Product No.	ETYP	MR (Miles)	EC (cc)	MS at month t (At)					
				A_1	A_2	A_3	A_4	A_5	A_6
1	IC	MR_1	$ECAP_2$	REP_1	REP_2		REL_1	REP_2	
2	IC	MR_1	$ECAP_2$	REP_1	REP_2		REL_1	REP_2	
3	IC	MR_1	$ECAP_1$			RP_2			
4	IC	MR_1	$ECAP_2$	REP_1	REP_2		REL_1	REP_2	
5	IC	MR_1	$ECAP_2$	REP_1	REP_2		REL_1	REP_2	REL_2
6	IC	MR_1	$ECAP_2$	REP_1	REP_2		REL_1	REP_2	REL_2
7	IC	MR_1	$ECAP_2$	REP_1	REP_2		REL_1	REP_2	REL_2
8	IC	MR_1	$ECAP_2$	REP_1	REP_2		REL_1	REP_2	REL_2
9	IC	MR_1	$ECAP_2$	REP_1	REP_2		REL_1	REP_2	
10	IC	MR_1	$ECAP_2$	REP_1	REP_2		REL_1	REP_2	
11	IC	MR_1	$ECAP_2$	REP_1	REP_2		REL_1	REP_2	REL_2
12	IC	MR_1	$ECAP_2$	REP_1					REL_2
13	HD	MR_1	$ECAP_1$		REP_2	REP_2		REL_2	
14	IC	MR_1	$ECAP_2$	REP_1	REP_2	REP_2	REL_1	REL_2	REL_2
15	HD	MR_1	$ECAP_1$			REP_2	REL_1	REL_2	
16	HD	MR_1	$ECAP_1$		REP_2		REL_1		
17	IC	MR_1	$ECAP_2$	REP_1	REP_2	REP_2	REL_1		REP_1
⋮	⋮	⋮	⋮	⋮	⋮	⋮	⋮	⋮	⋮
1071	HD	MR_1	$ECAP_1$	REP_1	REP_2		REL_1	REP_2	REL_2
1072	HD	MR_2	$ECAP_1$	REP_1	REP_2		REL_1	REP_2	REL_2
1073	IC	MR_1	$ECAP_1$		REP_2				REL_2
1074	IC	MR_1	$ECAP_2$	REP_1	REP_2		REL_1	REP_2	REL_2
1075	HD	MR_1	$ECAP_2$	REP_1	REP_2		REL_1		
1078	HD	MR_1	$ECAP_1$			REP_2			

| 1079 | HD | MR$_1$ | ECAP$_1$ | REP$_1$ | | REL$_1$ | REP$_2$ | REL$_2$ |
| 1080 | HD | MR$_1$ | ECAP$_1$ | REP$_1$ | | REL$_1$ | REP$_2$ | REL$_2$ |

Table 2. Description of MS on Car Engines and Tires.

Part No.	Part	Description	MS	
			Repair (REP)	Replace (REL)
1	Engine	Checking various engine components for necessary repairs or upgrades.	REP$_1$	REL$_1$
2	Tires	Inspecting wear or damage of tires to detect or predict if repairs or replacement of tires.	REP$_2$	REL$_2$

Table 3. Spare Parts For Car Engines and Tires.

SP	Engine	SP	Tires
S$_{11}$	Oil Pan	S$_{21}$	Tire sensor
S$_{12}$	Spark Plugs	S$_{22}$	Rotating tire
S$_{13}$	Oil filter	S$_{23}$	Spare tire
S$_{14}$	Head gasket		

Table 4. Spare Parts Replacements For Engines and Tires.

Replacement	Engine				Tires		
	S$_{11}$	S$_{12}$	S$_{13}$	S$_{14}$	S21	S22	S23
1	1	1	1	0	0	1	1
2	0	0	1	0	0	0	1
3	0	1	0	1	1	1	1
4	1	0	1	0	0	1	0
5	1	1	1	0	0	1	1
6	1	0	0	1	1	1	1
7	1	0	1	1	0	1	1
8	1	1	1	1	1	1	1
9	1	1	1	0	0	0	1
10	1	1	1	0	0	1	1
⋮	⋮	⋮	⋮	⋮	⋮	⋮	⋮
975	0	0	1	1	1	1	1
976	0	0	1	1	1	1	1
977	1	1	1	0	0	1	0
978	1	1	1	1	1	0	1
979	1	0	0	1	1	0	0
980	1	0	1	1	0	1	1

Prediction of monthly MS without car attributes

Firstly, the monthly MS data was analyzed without car attributes using data mining techniques as shown in Fig. 2. The generalized sequential pattern (GSP) technique was adopted to determine the frequent sequential patterns (SPs) between MS for 6 months as shown in Fig. 2. For month t, t=1, …, 6, a combination of the MS-related to engine and tires {REP_1t, REL_1t, REP_2t, REL_2t} were performed. Four possible activities can occur each month, resulting in 24 activities (n=24) that could take place. Table 5 shows all possible MS for each month.

Table 5. MS Data For Six Months.

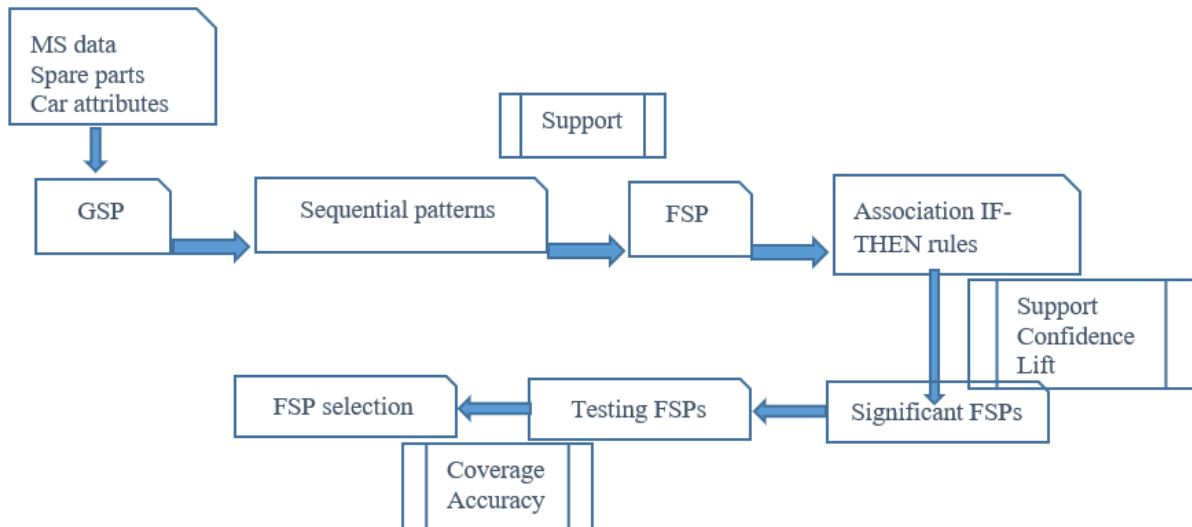| MS (At)					
A_1	A_2	A_3	A_4	A_5	A_6
REP_1	REP_1	REP_1	REP_1	REP_1	REP_1
REL_1	REL_1	REL_1	REL_1	REL_1	REL_1
REP_2	REP_2	REP_2	REP_2	REP_2	REP_2
REL_2	REL_2	REL_2	REL_2	REL_2	REL_2

Fig. 2. Data Mining Framework For Prediction of FSPs For MS.

Based on Table 5 and using Eq. (1), there resulted number (N) of possible sequential patterns of MS was 852 patterns.

$$N = n^2 + \frac{n(n-1)}{2} \tag{1}$$

The pattern's support value represents the pattern frequency according to all items and its threshold value of 40% [27]. Generally, an SP corresponding to a support value of at least 40% is judged a frequent sequential pattern (FSP). The support values were calculated using Eq. (2) and then the 2-item FSPs are listed in Table 6.

$$Sup\ (v_1 \rightarrow v_2) = \frac{|v_1 \cup v_2|}{|R|} \times 100\% \tag{2}$$

$|v_1 \cup v_2|$: the number of cars that contains event v_1 and event v_2.

$|R|$: the number of cars.

Table 6. The Best FSPs of MS.

Item-SFP	No.	FSP	Repeated pattern	Support (100%)
	1	$A_1 = REP_1, A_4 = REL_1$	680	63.0
2-item	2	$A_2 = REP_2, A_4 = REL_1$	680	63.0
	3	$A_1 = REP_1, A_2 = REP_2$	640	59.3
3-item	1	$A_1 = REP_1, A_2 = REP_2, A_4 = REL_1$	620	57.4

In Table 6, the FSP_2 was repeated for 680 cars; hence, the support value is 63.0%, indicating that 63.0% of automobiles had the sequential pattern ($A_1 = REP_1, A_4 = REL_1$). For the 2-item FSP, sequence ($A_1 = REP_1, A_4 = REL_1$) has the highest support value; however, the time between activities is three months. Also, sequence ($A_2 = REP_2, A_4 = REL_1$) corresponds to the highest support value, but the time between activities is two months. Therefore, ($A_1 = REP_1, A_4 = REL_1$) is the best sequence for the 2-item FSP. Further, a single 3-item pattern ($A_1 = REP_1, A_2 = REP_2, A_4 = REL_1$) is identified as FSP as shown in Table 6. Finally, all possible 4-item FSPs corresponded to support values smaller than 40% and consequently, they are not considered in further analysis.

Next, the IF-THEN rules are constructed to investigate the relationships between MS for the best 2-item and 3-item FSPs. The confidence value (a threshold value of 85%) is the probability that decision (DN) activities will occur given that condition (CN) activities occurred. Lift value (threshold value of 1) is the ratio of the joint probability of the activities to the expected joint probability if they are statistically independent. Significant rules correspond to a confidence value of more than 85% and a lift value larger than 1. Table 7 shows that association rules according to the best pattern for 2- and 3-item FSPs.

Table 7. Association Rules with the Best 2- and 3-item FSPs.

Item-FSP	Rule	CN	DN	Support (100%)	Confidence (100%)	Lift	Significance
3-item	1	$A_1 = REP_1$	$A_2 = REP_2, A_4 = REL_1$	57.4	86.1	1.37	Significant
	2	$A_1 = REP_1, A_2 = REP_2$	$A_4 = REL_1$	57.4	93.9	1.19	Significant
2-item	1	$A_1 = REP_1$	$A_2 = REP_2$	63.0	88.9	1.23	Significant

For rule 1 of the 3-item FSP with CN ($A_1 = REP_1$), DN ($A_2 = REP_2, A_4 = REL_1$), the support value is 57.4%. Confidence is then calculated using Eq. (3).

$$\text{Conf. (CN} \rightarrow \text{DN)} = \frac{|CN \cup DN|}{|CN|} \times 100\% \tag{3}$$

where

$|CN \cup DN|$: The number of cars (= 620) that contain CN ($A_1 = REP_1$) and DN ($A_2 = REP_2$, $A_4 = REL_1$). $|CN|$: The number of cars (= 720) that contain condition (Service1 = REP_1). Then,

Conf. (CN $\rightarrow$ DN) = $\times$ 100% = 86.1%

This means that when $A_1 = REP_1$ occurred, the FSP ($A_2 = REP_2$, $A_4 = REL_1$) had an occurrence probability of 86.1%. The Lift value (= 63 %) is then calculated using Eq. (4).

$$\text{Lift (CN} \rightarrow \text{DN)} = \frac{Sup\ (CN \cup DN)}{Sup\ (CN) \cdot Sup(DN)} \qquad (4)$$

$Sup\ (CN \cup DN)$ = Sup ($A_1 = REP_1$, $A_2 = REP_2$, $A_4 = REL_1$) is 57.4%. Moreover, $Sup\ (CN)$ = Sup ($A_1 = REP_1$) and $Sup\ (DN)$ = Sup ($A_2 = REP_2$, $A_4 = REL_1$) of 66.7 % and 63.0 %, respectively. Using Eq. (4), the lift is calculated as follows:

$$\text{Lift (CN} \rightarrow \text{DN)} = \frac{0.574}{0.667 \times 0.63} = 1.37$$

From Table 7, the listed three FSPs are significant rules that can be utilized in predicting the next MS. For illustration, for the 2-item FSP if REP_1 occurred in the first month ($A_1 = REP_1$), then the predicted maintenance service, A_2, in the second month is REP_2. Moreover, if ($A_1 = REP_1$, $A_2 = REP_2$) occurred, the predicted maintenance service, A_4, in the fourth month is REL_1.

Finally, the prediction accuracy for the significant relationships between the MS and attributes was evaluated using the testing data for 500 cars displayed in Table 8, where a single maintenance service can occur per month.

Table 8. Testing Data.

No.	ETYP	MR	ECAP	Monthly MS					
				A_1	A_2	A_3	A_4	A_5	A_6
1	IC	MR_1	$ECAP_2$	REP_1	REP_2		REL_1	REL_2	
2	IC	MR_1	$ECAP_2$	REP_1	REP_2		REL_1	REL_2	
3	IC	MR_1	$ECAP_1$			REP_2			
4	IC	MR_1	$ECAP_2$	REP_1	REP_2		REL_1	REL_2	
5	IC	MR_1	$ECAP_2$	REP_1	REP_2		REL_1	REL_2	REL_2
6	IC	MR_1	$ECAP_2$	REP_1	REP_2		REL_1	REL_2	REL_2
7	IC	MR_1	$ECAP_2$	REP_1	REP_2		REL_1	REL_2	REL_2
8	IC	MR_1	$ECAP_2$	REP_1	REP_2		REL_1	REL_2	REL_2
9	IC	MR_1	$ECAP_2$	REP_1	REP_2		REL_1	REL_2	
10	IC	MR_1	$ECAP_2$	REP_1	REP_2		REL_1	REL_2	
11	HD	MR_2	$ECAP_1$		REP_2				
12	HD	MR_1	$ECAP_1$			REL_1	REL_1	REP2	REL_2
13	HD	MR_1	$ECAP_1$		REP_2	REL_1	REL_1	REP2	REL_2
14	IC	MR_1	$ECAP_1$		REP_2	REL_1	REL_1	REP2	REL_2
15	HD	MR_1	$ECAP_1$			REL_1	REL_1	REP2	REL_2
16	HD	MR_2	$ECAP_1$			REL_1			

No.									
17	HD	MR₂	ECAP₁				REP2	REP₂	REL₂
18	HD	MR₂	ECAP₁				REP2	REP₂	REL₂
19	IC	MR₁	ECAP₂	REP₁				REP₂	REL₂
20	IC	MR₁	ECAP₁	REP₁	REP₂		REL₁	REP₂	REL₂
⋮	⋮	⋮	⋮	⋮	⋮		⋮	⋮	⋮
495	IC	MR₁	ECAP₂	REP1	REP₂		REL₁	REP₂	
496	IC	MR₁	ECAP₂	REP₁	REP₂		REL₁	REP₂	
497	HD	MR₂	ECAP₁		REP₂				
498	HD	MR₁	ECAP₁			REL₁	REL₁	REP₂	REL₂
499	IC	MR₁	ECAP₂	REP₁	REP₂		REL₁	REP₂	REL₂
500	IC	MR₁	ECAP₁	REP₁	REP₂				REL₂

The percentages of coverage (COV %) and accuracy (ACY %) were used to classify the data. The COV % is the percentage of the cars (N_s) that satisfy the CN of the rule in total number of cars (R) as given in Eq. (5).

$$COV = \frac{N_s}{R} \times 100\% \tag{5}$$

The ACY % is the percentage of the number (N_c) of CNs that satisfied the rule to the total number (N_s) of CN and DN that classified the rule as shown in Eq. (6).

$$ACY = \frac{N_c}{N_s} \times 100\% \tag{6}$$

A rule is considered accurate when COV% and ACY% are more than 40% and 85%, respectively. Table 9 shows the obtained prediction results from the testing data.

Table 9. Prediction Results of Testing Data.

No.	CN	DN	N_s	N_c	COV %	ACY %
1	$A_1 = REP_1$	$A_2 = REP_2$	320	300	64%	93.75%
2	$A_1 = REP_1$	$A_2 = REP_2, A_4 = REL_1$	320	280	64%	87.5%
3	$A_1 = REP_1, A_2 = REP_2$	$A_4 = REL_1$	300	280	60%	93.3%

The first rule indicates that if $A_1 = REP_1$ occurs, then $A_2 = REP_2$ will occur. From the testing data, for the first rule, $A_1 = REP_1 \rightarrow (A_1 = REP_1, A_2 = REP_2)$ the COV % and ACY % were 64.0% and 93.75%, meaning that service $A_1 = REP_1$ took place in 64.0 % of total cars in which the next maintenance service 93.75% was $A_2 = REP_2$. Consequently, the coverage and accuracy results indicate that the rules were predicted accurately.

Prediction of Monthly MS with Car Attributes

The GSPs for MS were generated with various combinations of car attributes (PY, ETYP, ECAP, and MR) with the best sequential patterns for 2- and 3-item FSPs given in Table 6. The threshold of support value was 25% [13]. Table 10 displays the 2- and 3-item FSPs for various car attributes. The GAPS were established to understand the relationships between MS and car attributes for the best FSPs as shown in Table 10.

From Table 10, four and five out of 12 rules were identified as insignificant for 2- and 3-item FSPs with car attributes, respectively. The testing data shown in Table 8 was adopted to evaluate COV % and ACY % of the significant rules. The obtained results are shown in Table 11, where the calculated COV % and ACY % indicate that all FSPs are accurately predicted.

Table 10. GAPS For the Best FSPs and Car Attributes.

Rule	CN	DN	Support (100%)	Conf. (100%)	Lift	Sig.
2-item FSP						
1	CAP_2	$A_1 = REP_1, A_2 = REP_2$	53.7	96.6	1.59	Yes
2	CAP_2, IC	$A_1 = REP_1, A_2 = REP_2$	46.3	96.0	1.59	Yes
3	M_1, CAP_2	$A_1 = REP_1, A_2 = REP_2$	44.4	88.5	1.46	Yes
4	M_1, IC	$A_1 = REP_1, A_2 = REP_2$	44.4	82.1	1.36	No
5	M_1	$A_1 = REP_1, A_2 = REP_2$	38.9	54.0	0.9	No
6	IC	$A_1 = REP_1, A_2 = REP_2$	35.2	79.1	1.26	No
7	CAP_2	$A_1 = REP_1, A_2 = REP_2$	38.9	95.2	1.59	Yes
8	IC, CAP_2, M_1	$A_1 = REP_1, A_2 = REP_2$	40.7	95.5	1.59	Yes
9	IC, CAP_2	$A_1 = REP_1, A_2 = REP_2$	37.0	95.0	1.59	Yes
10	M_1, CAP_2	$A_1 = REP_1, A_2 = REP_2$	37.0	95.0	1.59	Yes
11	IC, M_1	$A_1 = REP_1, A_2 = REP_2$	35.2	78.2	1.31	No
12	IC, M, CAP_2	$A_1 = REP_1, A_2 = REP_2$	33.3	94.7	1.50	Yes
3-item FSP						
1	CAP_2	$A_1 = REP_1, A_2= REP_2, A_4 = REL_1$	50.0	93.1	1.62	Yes
2	CAP_2, IC	$A_1 = REP_1, A_2 = REP_2, A_4 = REL_1$	42.6	92.0	1.60	Yes
3	M_1, CAP2	$A_1= REP_1, A_2 = REP_2, A_4 = REL_1$	40.7	84.6	1.47	No
4	M_1, IC	$A_1 = REP_1, A_2 = REP_2, A_4 = REL_1$	40.7	78.6	1.37	No
5	M_1	$A_1 = REP_1, A_2 = REP_2, A_4 = REL_1$	40.7	59.5	1.03	No
6	IC	$A_1 = REP_1, A_2 = REP_2, A_4 = REL_1$	37.0	83.3	1.45	No
7	CAP_2	$A_1 = REP_1, A_2 = REP_2, A_4 = REL_1$	37.0	95.2	1.66	Yes
8	IC, CAP_2, M_1	$A_1 = REP_1, A_2 = REP_2, A_4 = REL_1$	37.0	90.9	1.58	Yes

9	IC, CAP_2	$A_1 = REP_1, A_2 = REP_2, A_4 = REL_1$	35.2	95.0	1.66	Yes
10	M_1, CAP_2	$A_1 = REP_1, A_2 = REP_2, A_4 = REL_1$	35.2	95.0	1.66	Yes
11	IC, M_1	$A_1 = REP_1, A_2 = REP_2, A_4 = REL_1$	33.3	78.2	1.36	No
12	IC, M_1, CAP_2	$A_1 = REP_1, A_2 = REP_2, A_4 = REL_1$	33.3	94.7	1.65	Yes

Prediction of Spare Part Replacement

The data for spare part replacements are analyzed as follows. According to Table 3, spare parts were recorded for the engine and tires. GSP for the related spare parts of engine and tires (REL_1, REL_2) to know frequent spare parts for each service. The support threshold was determined 40% based on the manufacturer and expert opinion. Replacement service REL_1 had spare parts ($S_{11}, S_{12}, S_{13}, S_{14}$) , so four possible spare parts for REL_1 ($n=4$). The number of possible patterns (= 22) is calculated using Eq. (1). Table 12 displays the FSPs of spare part replacements. Similarly, replacement service REL_2 had (S_{21}, S_{22}, S_{23}) spare parts, so three possible spare parts for REL_2 ($n=3$). The number of possible patterns (= 12) was calculated using Eq. (1). The best FSP is the sequence containing the highest number of spare parts with the highest acceptable support value larger than 40%. Consequently, the FSPs (S_{12}, S_{13}, S_{14}) and (S_{21}, S_{22}, S_{23}) were chosen as the best FSPs for spare part replacements REL_1 and REL_2, respectively.

Table 11. Prediction Results of Significant Rules of MS with Attributes.

No. of rule	CN	DN	N_s	N_c	COV %	ACY %
1	CAP_2	$A_1 = REP_1, A_2 = REP_2, A_4 = REL_1$	280	260	56%	92.86%
2	CAP_2, IC	$A_1 = REP_1, A_2 = REP_2, A_4 = REL_1$	260	240	52%	92.31%
3	CAP_2	$A_1 = REP_1, A_2 = REP_2, A_4 = REL1$	260	240	52%	92.31%
4	IC, CAP_2, M_1	$A_1 = REP1, A_2 = REP2, A_4 = REL_1$	240	220	48%	91.67%
5	IC, CAP_2	$A_1 = REP_1, A_2 = REP_2, A_4 = REL_1$	260	240	52%	92.31%
6	M_1, CAP_2	$A_1 = REP_1, A_2 = REP_2, A_4 = REL_1$	240	220	48%	91.67%
7	IC, M_1, CAP_2	$A_1 = REP_1, A_2 = REP2, A_4 = REL_1$	240	220	48%	91.67%

8	CAP_2	$A_1 = REP_1, A_2 = REP_2$	280	260	56%	92.86%
9	CAP_2, IC	$A_1 = REP_1, A_2 = REP_2$	260	240	52%	92.31%
10	M_1, CAP_2	$A_1 = REP_1, A_2 = REP_2$	240	220	48%	91.67%
11	CAP_2	$A_1 = REP_1, A_2 = REP_2$	260	240	52%	92.31%
12	IC, CAP_2, M_1	$A_1 = REP_1, A_2 = REP_2$	240	220	48%	91.67%
13	IC, CAP_2	$A_1 = REP_1, A_2 = REP_2$	260	240	52%	92.31%
14	M_1, CAP_2	$A_1 = REP_1, A_2 = REP_2$	240	220	48%	91.67%
15	IC, M_1,, CAP_2	$A_1 = REP_1, A_2 = REP_2$	240	220	48%	91.67%

Table 12. FSPs of Spare Part Replacements for Engine and Tires.

Pattern	FSP	Items	Repeated patterns	Support (100%)
Engine				
1	S_{12}, S_{13}	2	374	55.0
2	S_{12}, S_{14}	2	442	65.0
3	S_{13}, S_{14}	2	408	60.0
4	S_{11}, S_{12}, S_{14}	3	374	55.0
Tires				
1	S_{21}, S_{23}	2	539	55.0
2	S_{22}, S_{23}	2	490	50.0
3	S_{21}, S_{22}, S_{23}	3	441	45.0

Results

From Table 6, the best 3-item FSP without car attributes was ($A_1 = REP_1$, $A_2 = REP_2$, $A_4 = REL_1$). The integration of this FSP with various car attributes and the FSP (S_{11}, S_{12}, S_{14}) for engine spare part replacement service is depicted in Fig. 3. Similarly, the maintenance prediction with a 2-item FSP ($A_1 = REP_1$, $A_2 = REP_2$) shown in Table 6 is depicted in Fig. 4.

This research proposed an integrated data-mining framework for predicting the significant FSPs for cars under warranty for the following cases: (a) the monthly MS with product attributes, (b) the monthly MS with product attributes, (c) the spare part replacement, and (d) the monthly MS with product attributes and spare part replacements. The results showed that:

(a) For the monthly MS without car attributes, the best 3-item FSPs are ($A_1 = REP_1$, $A_2 = REP_2$, $A_4 = REL_1$) of support, confidence, and lift values of 57.4 %, 93.9 %, and 1.19, respectively. The predicted maintenance sequence is engine repair in the first month followed by tire repair in the second month, and spare part replacements of car engines in the fourth month.

(b) The product attributes with the best 3-item FSPs were (A_1 = REP$_1$, A_2 = REP$_2$, A_4 = REL$_1$), the significant FSPs are (CAP$_2$), (CAP$_2$, IC), (2021, CAP$_2$), (IC, CAP$_2$, M$_1$), (2021, IC, CAP$_2$), (2021, M$_1$, CAP$_2$), (2021, IC, M$_1$, CAP$_2$) of confidence % (COV %, ACY %) of 93.1 % (56 %, 92.86 %), 92 % (52 %, 92.31 %), 95.2 % (52 %, 92.31 %), 90.9 % (48 %, 91.67 %), 95 % (52 %, 92.31 %), 95 % (48 %, 91.67 %), and 94.7 % (48 %, 91.67 %), respectively. Cars with engine capacity (C$_2$) of more than 1800 cc have the highest probability in all significant FSPs. Moreover, significant FSPs were observed for MS cars with internal combustion (IC) engines with a capacity of more than 1800 cc or travelled more than 18000 miles.

(c) For the prediction of FSPs of spare part replacements, the best significant FSPs for spare part replacement corresponding to car engines and tires are (S$_{12}$, S$_{13}$, S$_{14}$) and (S$_{21}$, S$_{22}$, S$_{23}$) with support values of 55 % and 45 %, respectively.

(d) In the integrated prediction of significant FSPs, about 15 significant 2- and 3-item FSPs are identified as shown in Figs. 3 and 4.
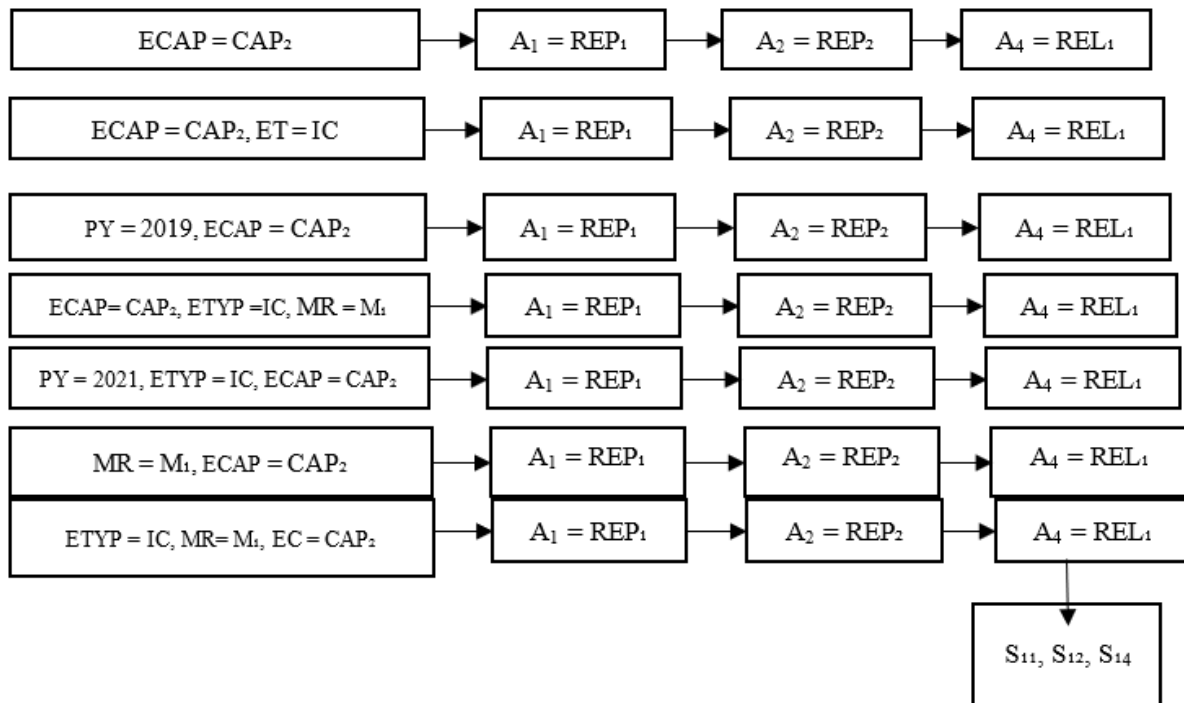
Fig. 3. The Integrated Prediction of 3-item FSPs for MS.

The prediction results can help maintenance service centers reduce the economic losses due to inefficient planning and poor performance of MS. Inventory control engineering can utilize the proposed data-mining framework to predict FSPs of MS in planning and prioritizing spare parts' inventory levels effectively and utilizing maintenance resources efficiently. In return, the results may lead to reduced maintenance costs, enhancing customer satisfaction, and achieving a competitive advantage in the maintenance of recalled cars
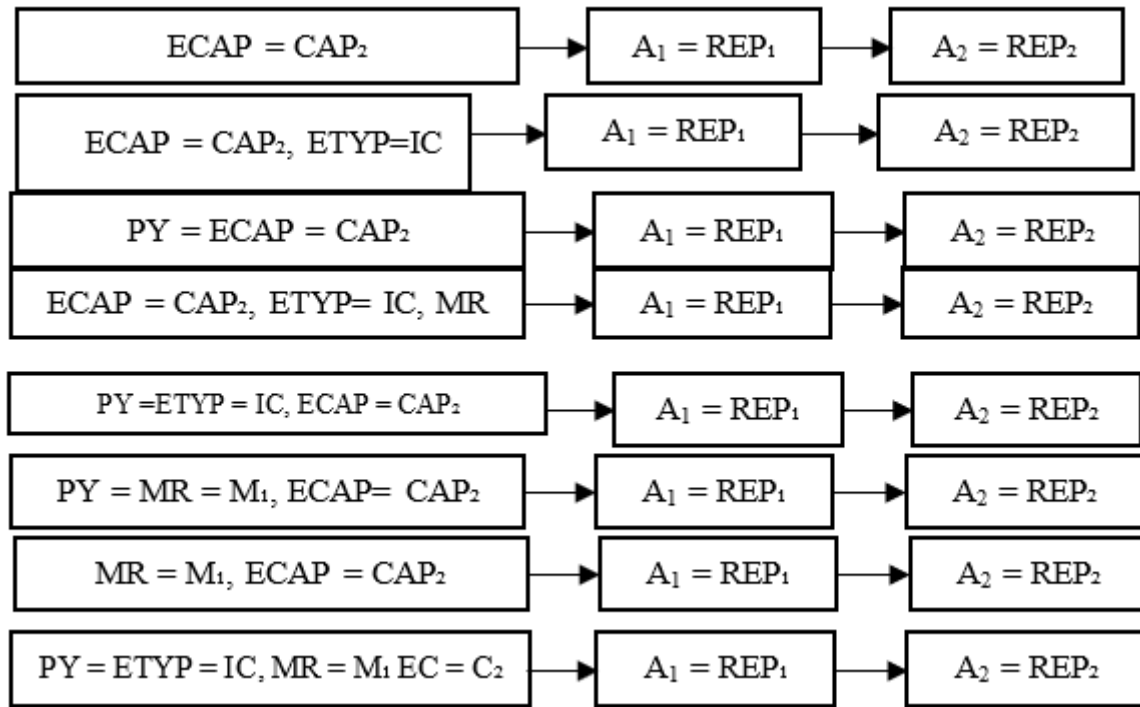
under warranty.

Fig. 4. The Maintenance Prediction with A 2-item FSP.

Conclusion

Maintenance services are crucial to automobile market growth. In practice, failure occurrence time, type, and needed spare parts are uncertain. This requires effective and efficient MS. This research, therefore, utilized data mining techniques to predict the significant FSPs for MS including spare part replacements for cars under warranty. Data on MS was obtained from a recorded database for 1080 cars with 980 spare part replacements recorded over six months. Various data mining tools were used for analyzing and validating the significant FSPs with and without car attributes including; production year, engine type and capacity, and mileage for repair. Moreover, significant FSPs were determined for spare part replacements. Finally, concurrent prediction of FSPs for MS with spare part needs was established. The results revealed that the predicted significant FSP for MS is engine repair in the first month, tire repair in the second month, and spare part replacements of car engines in the fourth month. The significant FSPs of the next MS with car attributes revealed that more focus should be directed to engine capacity (CAP_2) of more than 1800 cc, cars with internal combustion (IC) and CAP_2 engines travelled more than 18,000 miles. In conclusion, the resulting significant FSPs may support maintenance engineering to reduce maintenance and inventory costs, improve customer satisfaction, and enhance the competitive advantage of cars under warranty. Future research considers using data mining techniques to predict significant FSPs with more car attributes and MS.

References

Al-Refaie, A., & Aljundi, H. (2024). A Fuzzy FMEA-Resilience Approach for Maintenance Planning in a Plastics Industry. International *Journal of Prognostics and Health Management*, 15(2).

Al-Refaie, A., & Al-Hawadi, A. (2023). A proposed eFSR blockchain system for optimal planning of facility services with probabilistic arrivals and stochastic service durations. *Buildings*, 13(1), 240.

Al-Refaie, A., & Almowas, H. (2023). Multi-objective maintenance planning under preventive maintenance. *Journal of Quality in Maintenance Engineering*, 29(1), 50-70.

Al-Refaie, A., Ghaleb Abbasi, G., & Al-Hawadi, A. (2023). DEA Efficiency Assessment of Packaging Lines in A Pharmaceutical Industry. *Eng. Lett*, 31, 1241-1249.

Al-Refaie, A., & Al-Hawadi, A. (2022). Optimal fuzzy repairs' scheduling and sequencing of failure types over multiple periods. *Journal of Ambient Intelligence and Humanized Computing*, 13(1), 201-217.

Al-Refaie, A., Al-Hawadi, A., & Lepkova, N. (2022). Blockchain design with optimal maintenance planning. *Buildings*, 12(11), 1902.

Al-Refaie, A., Al-Shalaldeh, H., & Lepkova, N. (2020). Proposed procedure for optimal maintenance scheduling under emergent failures. *Journal of Civil Engineering and Management*, 26(4), 396-409.

Al-Refaie, A., & Hanayneh, B. (2014). Influences of TPM, TQM, Six Sigma practices on firms performance in Jordan. *International Journal of Productivity and Quality Management*, 13(2), 219-234.

Al-Refaie, A., Abu Hamdieh, B., & Lepkova, N. (2023). Prediction of maintenance activities using generalized sequential pattern and association rules in data mining. *Buildings*, *13*(4), 946.

Al-Refaie, A., & Hamdieh, B. A. (2024). A Data Mining Framework for Maintenance Prediction of Faulty Products Under Warranty. *Journal of Advanced Manufacturing Systems*, *23*(1).

Astuti, J., & Yuniarti, T. (2023). Data Mining Modeling in Clustering Car Products Sales Data in the Automotive Industry in Indonesia. *Jurnal Manajemen Industri dan Logistik*, *7*(2), 261-281.

Awwalu, J., Ghazvini, A., & Bakar, A. A. (2014). Performance comparison of data mining algorithms: a case study on car evaluation dataset. *Int. J. Comput. Trends Technol*, *13*(2), 78-82.

Bastos, P., Lopes, I., & Pires, L. (2014). Application of data mining in a maintenance system for failure prediction. *Safety, Reliability and Risk Analysis: Beyond the Horizon: 22nd European Safety and Reliability*, *1*, 933-940.

Bastos, P., Lopes, I. D. S., & Pires, L. (2012). A maintenance prediction system using data mining techniques. Proceedings of the World Congress on Engineering Vol III WCE 2012, July 4 - 6, 2012, London, U.K.

Buddhakulsomsiri J. & Zakarian A. (2009). Sequential pattern mining algorithm for automotive warranty data. *Comput. Ind. Eng. 57*, 137–147.

Buddhakulsomsiri, J.; Siradeghyan, Y.; Zakarian, A.; Li, X. (2006). Association rule-generation algorithm for mining automotive warranty data. *Int. J. Prod. Res. 44*, 2749–2770.

Chen, C., Liu, Y., Sun, X., Di Cairano-Gilfedder, C., & Titmus, S. (2021). An integrated deep learning-based approach for automobile maintenance prediction with GIS data. *Reliability Engineering & System Safety*, *216*, 107919.

ICTELS

International Conference on
Technology, Engineering, and
Life Sciences

iSTES

www.ictels.net   May 16-19, 2025   Rome, Italy   www.istes.org

Cheng, K., Sun, D., Chen, C., Qin, D., & Wang, K. (2022). Intelligent gear decision method for automatic vehicles based on data mining under uphill conditions. *IEEE Transactions on Intelligent Transportation Systems*, *23*(12), 24235-24247.

Hartung, J., Gühring, G., Licht, V., & Warta, A. (2020). Comparing multidimensional sensor data from vehicle fleets with methods of sequential data mining. *SN Applied Sciences*, 2(4), 709.

İfraz, M., Ersöz, S., Aktepe, A., & Çetinyokuş, T. (2024). Sequential predictive maintenance and spare parts management with data mining methods: a case study in bus fleet. *The Journal of Supercomputing*, 1-25.

Jacobs, J.A.; Mathews, M.J.; Kleingeld, M. (2019). Failure Prediction of Mine Compressors. *J. Fail. Anal. Prev. 19*, 976–985.

Llopis-Albert C., Rubio F., and Valero F.(2021). Impact of digital transformation on the automotive industry. *Technol. Forecast. Soc. Change*, 162, 120343. doi: 10.1016/j.techfore.2020.120343.

Moharana, U. C., & Sarmah, S. P. (2015). Determination of optimal kit for spare parts using association rule mining. *International Journal of System Assurance Engineering and Management*, *6*, 238-247.

Moharana, U., Sarmah, S., Rathore, P.K. (2019). Application of data mining for spare parts information in maintenance schedule: A case study. *J. Manuf. Technol. Manag. 30*, 1055–1072.

Rasheed, M. A. A. (2014). Adoption of data mining technique to find the condition of an automobile machine. *International J. Inf. Syst. Eng,* 2(1), 13-19.

Patel, J.K. (2021). The importance of equipment maintenance forecasting. *Int. J. Mech. Eng. 8*, 7–11.

Prytz, R., Nowaczyk, S., Rögnvaldsson, T., & Byttner, S. (2013). Analysis of truck compressor failures based on logged vehicle data. In *9th International Conference on Data Mining, Las Vegas, Nevada, USA, July 22–25, 2013*. CSREA Press.

Romelfanger M. and Kolich M. (2019). Comfortable automotive seat design and big data analytics: A study in thigh support. *Appl. Ergon.,* 75, 257–262. doi: 10.1016/j.apergo.2018.08.020.

Romanowski, C. J., & Nagi, R. (2001). Analyzing maintenance data using data mining methods. In *Data Mining for Design and Manufacturing: Methods and Applications* (pp. 235-254). Boston, MA: Springer US.

Salmi, M., & Atif, D. (2021). Using a data mining approach to detect automobile insurance fraud. In *International Conference on Soft Computing and Pattern Recognition* (pp. 55-66). Cham: Springer International Publishing

Simmachan, T., Manopa, W., Neamhom, P., Poothong, A., & Phaphan, W. (2023). Detecting fraudulent claims in automobile insurance policies by data mining techniques. *Thailand Statistician*, *21*(3), 552-568.

Srinivasan, R., Manivannan, S., Ethiraj, N., Devi, S. P., & Kiran, S. V. (2016). Modelling an optimized warranty analysis methodology for fleet industry using data mining clustering methodologies. *Procedia Computer Science*, *87*, 240-245.

Teo, H. G. (2010). *Data mining in automotive warranty analysis* (Doctoral dissertation, Open Access Te Herenga Waka-Victoria University of Wellington).

Wang C. J. and Kim B. G. (2020). Automotive Big Data Pipeline: Disaggregated HyperConverged Infrastructure vs Hyper-Converged Infrastructure. Proc. - 2020 IEEE Int. Conf. Data, Big Data 10.1109/BigData50022.2020.9378045.

Wakiru, J., Pintelon, L., Muchiri, P., & Chemweno, P. (2021). A data mining approach for lubricant-based fault diagnosis. *Journal of Quality in Maintenance Engineering*, 27(2), 264-291.

Xu, X., & Gui, M. (2021). Applying data mining techniques for technology prediction in new energy vehicle: a case study in China. *Environmental Science and Pollution Research*, *28*, 68300-68317.

Zabinski, K., Shubenkova, K., Makarova, I., & Zielosko, B. (2021, November). Car Safety Support System on the Base of Data Mining Algorithm. In Second Conference on Sustainable Development: Industrial Future of Territories (IFT 2021) (pp. 335-341). Atlantis Press.

Automobile Windshield Wipers Fluid System Design and Analysis- A Mechanical Engineering Undergraduate Students Design Project

Jay Albayyari

Wright State University, USA

Abstract: This research provides a fundamental study of the fluid mechanics of an automobile washer spray system from the reservoir to the windshield. Having properly working windshield wipers is one of the most overlooked features of being safe while driving. Whether it's dealing with poor weather conditions or other obstructions, efficient windshield wipers are key to having the clearest view while driving. It features wiper blades with holes that produce a highly precise spray of washer fluid directly in front of the moving wipers. The system helps eliminate the brief, vision-blocking spray across the full windshield that happens with most vehicles. Washer and wiper are combined into the blade to replace conventional spray nozzles. A duct system will take washer fluid directly to the wiper blade, where the wiper fluid is sprayed out from many small holes. The fluid will be precisely ejected to the front of the wipers and onto the windshield and the wiper blade at the same time will sweep across the surface to in either direction. This aim of work is described in this paper, fluid design and analysis of windshield wiper system in an automobile using fluid mechanics principles[1-2]. The design will include analysis of an existing automobile windshield wipers fluid systems and how to improve the system.

Keywords: Fluid Mechanics, Windshield Wiper System, Washer Spray, Automobile Design, Flow Analysis

Inroduction

Mary Anderson patented the windshield wiper idea in 1903 at the age of 37 were Few people saw the need for windshield wipers at the time, as automobiles were not common. Companies did not see the product as profitable and didn't want to mass produce it as concerns were raised about the wipers distracting drivers and causing accidents. A few years later in 1908, Henry Ford included windshield wipers on the Model T automobile, and all automobiles had them a few years later.

In this paper will look at the existing design of a windshield wiper fluid system for a Honda 2007 CRV and how to improve it. The study using fluid mechanics equations will analyze the work required by the system pump

for the current design, rough pipes design, and alternate design. The results of the three models will be compared.

Until todays automobile manufacturers are continuously looking for ways to improve windshield wipers systems to make them more effective and cheaper to manufacture. For example, prototyped in 2013, Mercedes Benz was the first company to incorporate wiper blades with integrated washer fluid nozzles, which spray fluid directly onto the windshield through integrated nozzles on both sides of the wipers. The design is currently used for high end car models because it is more expensive but, in the future, after they figure out how to reduce the cost of it to make it more affordable, they will be more common on vehicles.

Nomenclature

Re	Reynolds Number
V_{ave}	Fluid Velocity
D_h	Hydraulic Diameter
v	Viscosity
L	Tube Length
Z	Elevation
f	Friction Factor
h_L	Head losses
g	Gravitational Acceleration
h_{pump}	Pump Head
P	Pressure
ρ	Density
W_{pump}	Pump Work
n_{pump}	Pump Efficiency
K_L	Minor Losses
$h_{turbine}$	Turbine Head

Analysis

The following equations will be used to analyze the windshield wiper fluid system shown in figure 1:

$$Re = \frac{V_{ave} D_h}{v}$$

$$h_{L,Total} = h_{L,Major} + h_{L,Minor} = \sum f \frac{L}{D} \frac{V_{ave}^2}{2g} + \sum K_L \frac{V_{ave}^2}{2g}$$

$$\frac{P_1}{\rho g} + \frac{V_1^2}{2g} + z_1 + h_{pump} = \frac{P_2}{\rho g} + \frac{V_2^2}{2g} + z_2 + h_{turbine} + h_L$$
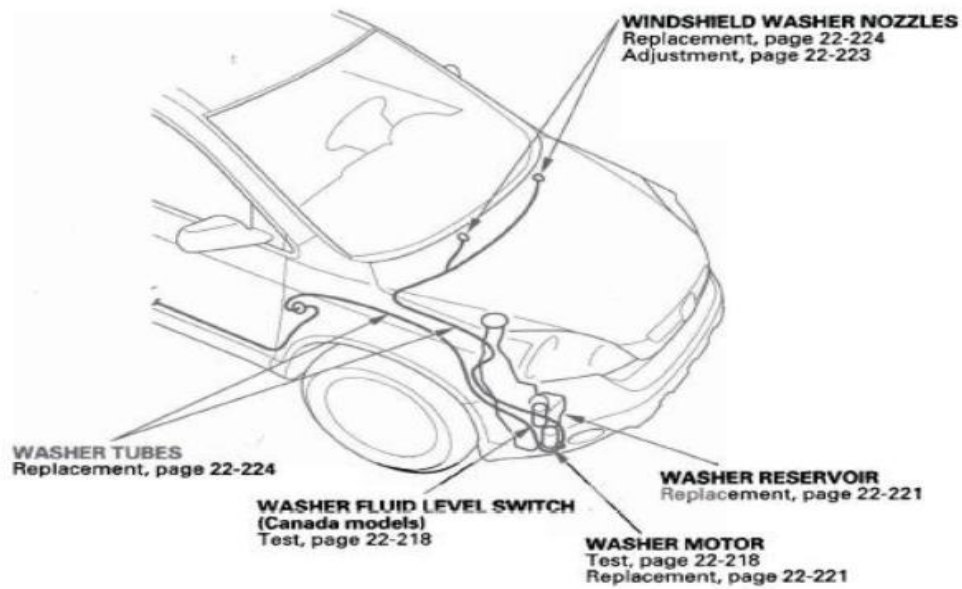
$$W_{pump} = \frac{h_{pump} mg}{n_{pump}}$$
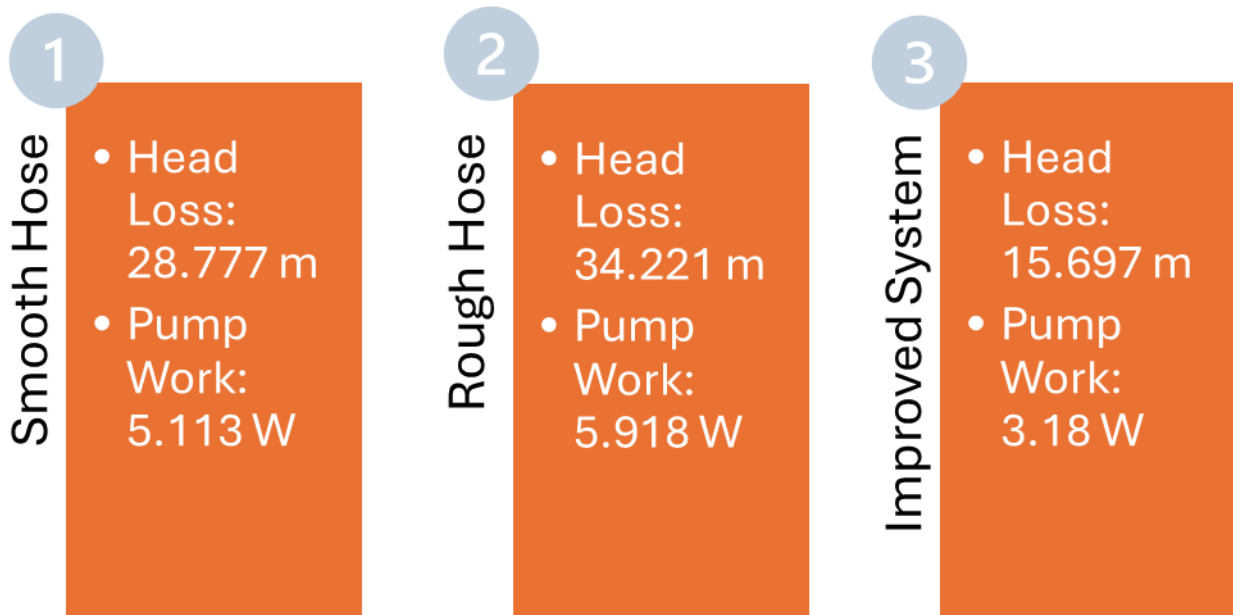

Figure 1. Honda CRV Windshield Wiper Fluid System

1
Smooth Hose
- Head Loss: 28.777 m
- Pump Work: 5.113 W

2
Rough Hose
- Head Loss: 34.221 m
- Pump Work: 5.918 W

3
Improved System
- Head Loss: 15.697 m
- Pump Work: 3.18 W

Figure 2. Three Designs Analysis Results

The results of the analysis (Figure 2) shows the difference in head loss and necessary pump work when using a smooth hose and rough hose with the current setup, as well as a smooth hose with our improved setup. As you can see, rough hoses are not used in washer fluid systems because it requires more pump work and results in more friction losses. The comparison also shows how much our changes would improve the efficiency of the washer fluid system.

Conclusion

This comparison shows the difference in head loss and necessary pump work when using a smooth hose and rough hose with the current setup, as well as a smooth hose with our improved setup. As you can see, rough hoses are not used in washer fluid systems because it requires more pump work and results in more friction losses. The comparison also shows how much the improved system changes would improve the efficiency of the washer fluid system.

References

Cengel, Y. A., & Cimbala, J. M. (2017). *Fluid mechanics: Fundamentals and applications* (4th ed.). McGraw-Hill Education.

Munson, Bruce Roy, 1940-. Fundamentals of Fluid Mechanics. Hoboken, NJ: John Wiley & Sons, Inc., 2013.

Electric Field Derived from the Potential of a Uniform Ring of Charge

Bendaoud Saâd

Cadi Ayyad University, National School of Applied Sciences of Safi, MISCOM Laboratory,

Sidi Bouzid's road, PO Box 63, Safi, Morocco 46000

Abstract: The uniformly charged ring is a classic electrostatics problem, providing a simple model for complex charge distributions. Although it is straightforward to calculate the electric field along the axis of the ring, analytical solutions at an angle to the axis are more challenging and are often omitted from standard curricula. This work provides a comprehensive derivation of the electrostatic potential and field at an arbitrary point in space for a uniformly charged ring. Formulating the potential in cylindrical coordinates and applying the gradient operator yields exact expressions for the radial and axial field components in closed form, articulated in terms of complete elliptic integrals of the first and second kinds. In addition to presenting the analytical solution, we emphasize the significant pedagogical value of this problem as an integrative exercise in potential theory, vector calculus, and the application of special functions. Furthermore, we demonstrate the relevance of the results to modern technologies, including quadrupole mass spectrometers, particle accelerator storage rings, and atomic force microscopes. This analysis reaffirms the enduring value of the charged ring model as a critical nexus between theoretical physics education and applied engineering.

Keywords: Uniformly charged ring, Ring of charge, Electric potential, Electric field, Elliptic integrals.

Introduction

In electrostatics, the pedagogical progression typically begins with discrete charge distributions, advancing to continuous ones only after the foundational principles, such as Coulomb's law and electric potential, have been established. To make these more complex calculations tractable, instruction heavily relies on case studies with high degrees of symmetry—such as infinite lines, spheres, and cylinders—where Gauss's law yields straightforward solutions for the electric field. Consequently, standard textbooks often ignore asymmetric cases. A prime example is the uniformly charged ring, the field of which is almost exclusively derived along its symmetry axis (Plonus, 1978; Serway & Jewett, 2014; Young & Freedman, 2012). However, the general off-axis problem presents a significant analytical challenge that remains largely absent from core curricula, despite its considerable value. The literature confirms both the complexity and the enduring interest in this problem. Early work by Zypman (2006) provided a treatment of the off-axis field, while Mandre (2007) expressed the field components in terms of complete elliptic integrals, albeit through laborious calculations. Ciftja et al. (2009)

subsequently derived the off-axis potential via direct integration, paving the way for the field to be obtained through differentiation. Further contributions, including simplified pedagogical approaches by Wissner-Gross (2012) and analyses of non-centred rings by Escalante (2021), have enriched the discussion. Furthermore, this problem is not just theoretical; it has applications in technologies such as scanning force microscopy (Eisenberg & Zypman, 2019; Gordon et al., 2024; Lazarev & Zypman, 2017). Related asymmetric configurations, including charged disks (Bochko & Silagadze, 2020; Martín-Luna & al., 2023; Sagaydak & Silagadze, 2024) and annular geometries (Ciftja, 2023; Ciftja & Bentley, 2024), share similar computational difficulties.

This study synthesizes and extends these previous efforts to present a unified and pedagogically robust framework for the off-axis electrostatics of a charged ring. We argue that a thorough analysis of symmetry and invariance (Boridy, 2005; Pérez et al., 2002; Ulaby, 2007) is essential for rigorous calculations. In line with engineering best practices, we validate our results through two complementary methods: firstly, by directly calculating the potential and applying the gradient operator; and secondly, by leveraging its governing differential equation. The resulting field components are expressed concisely in terms of complete elliptic integrals of the first and second kinds, with the third kind appearing naturally in the differential equation approach when the characteristic parameter equals the squared modulus. This work's primary contribution is a novel pedagogical approach that integrates potential theory, vector calculus, and special functions such as complete elliptic integrals. By presenting a reliable method of deriving the field from the potential for a canonical asymmetric problem, we equip educators with a valuable resource for overcoming a substantial shortcoming in traditional electrostatics teaching.

Materials, Methods, and Calculus of the Potential of the Ring

Consider a ring of radius R, with total charge Q uniformly distributed along its circumference. The position vector $\boldsymbol{r}$ to a point P, for which the potential $V(\boldsymbol{r})$ and electric field $\mathbf{E}(\boldsymbol{r})$ are to be determined, is shown in **Fig**. 1.
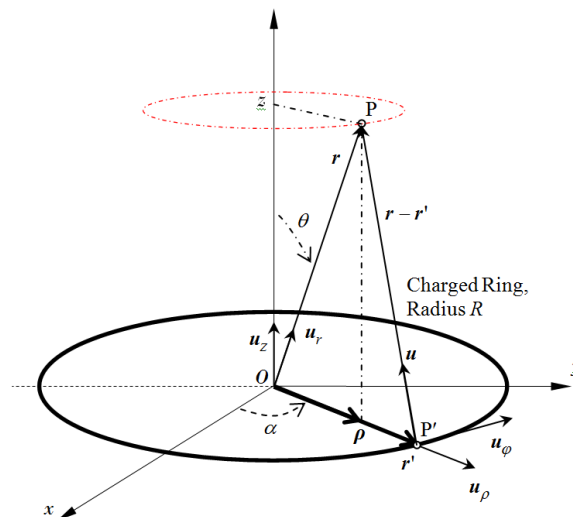

Figure 1. The ring lies on the *xy* plane. The field point P has cylindrical coordinates (ρ, *z*).

International Conference on
Technology, Engineering, and
Life Sciences

ICTELS

iSTES

www.ictels.net   May 16-19, 2025   Rome, Italy   www.istes.org

The elemental electric potential $dV(r)$ at a point P in space, arising from an infinitesimal charge segment dq located at the source point P′ on the ring, is given by Coulomb's law (Plonus, 1978; Boridy, 2005; Pérez et al., 2002):

$$dV(r) = k_e \frac{dq}{\|r - r'\|} \tag{1}$$

where $k_e = 1/(4\pi\varepsilon_0)$ is Coulomb's constant, $\varepsilon_0 = 8.845 \times 10^{-12}$ F.m^{-1} is the vacuum permittivity, r' is the vector position from dq to P, and $r - r'$ is the displacement vector pointing from point P′ to P.

The small charge element dq at point P′ on the ring can be described in Cartesian coordinates as follows:

$$r' = R \cos \alpha \, i + R \sin \alpha \, j \tag{2}$$

where α is the azimuthal angle measured from the x axis.

The position vector r can be expressed in cylindrical coordinates from the spherical coordinates in the ρz plane as follows:

$$\begin{aligned} r &= r u_r \\ &= \rho \, u_\rho + z \, u_z \end{aligned} \tag{3}$$

with

$$\cos(\theta) = \frac{r.k}{r} \text{ , we get: } \rho = r \sin \theta \text{ , and } z = r \cos \theta \tag{4}$$

Due to the system's axial symmetry, the potential $V(r)$ is independent of the azimuthal angle φ of the field point in cylindrical coordinates (ρ, φ, z). Therefore, the potential at any point depends only on the coordinates (ρ, z) and the calculation can be performed in the xz plane (where $\varphi = 0$) without loss of generality.
In this plane, the position vector of the field point simplifies to:

$$r = \rho \, i + z \, k \tag{5}$$

The displacement vector from the source element dq at P′ to the field point P is: $r - r'$.
Using Eqs. (2) and (5), its magnitude is given by:

$$\|r - r'\| = (R^2 + \rho^2 + z^2 - 2R\rho \cos \alpha)^{1/2} \tag{6}$$

When Eq. (6) is substituted into Eq. (1), the potential becomes:

$$dV(r) = k_e \frac{dq}{(R^2 + \rho^2 + z^2 - 2R\rho\cos\alpha)^{1/2}} \tag{7}$$

From this point onwards, there is no need to restrict the calculation to the *xz* plane. Instead, any ρz plane can be considered by symmetry, i.e., any angle φ. For a uniformly charged ring, the linear charge density is constant, $\lambda = Q/(2\pi R)$, so $dq = \lambda R d\alpha = (Q/(2\pi))d\alpha$. Substituting this in Eq. (7) and integrating over the ring's circumference, the total potential is:

$$V(\rho, z) = k_e \frac{Q}{2\pi} \int_0^{2\pi} \frac{d\alpha}{(R^2 + \rho^2 + z^2 - 2R\rho\cos\alpha)^{1/2}} \tag{8}$$

This integral can be expressed in terms of a complete elliptic integral of the first kind. By exploiting the periodicity of the cosine function, the integral can be rewritten as follows:

$$V(\rho, z) = k_e \frac{Q}{\pi} \int_0^{\pi} \frac{d\alpha}{(R^2 + \rho^2 + z^2 - 2R\rho\cos\alpha)^{1/2}} \tag{9}$$

Integration by substitution should be used, and the integration variable should be changed according to the following:

$$\beta = \frac{\pi - \alpha}{2}, \text{ such that, } \alpha = \pi - 2\beta, \ d\alpha = -2d\beta \tag{10}$$

$$\alpha = 0 \to \beta = \frac{\pi}{2}, \ \alpha = \pi \to \beta = 0, \ \cos(\alpha) = \cos(\pi - 2\beta) = -\cos(2\beta) = 2\sin^2(\beta) - 1 \tag{11}$$

Substituting this into function (9) gives:

$$V(\rho, z) = k_e Q \frac{2}{\pi} \int_0^{\pi/2} \frac{d\beta}{(\rho^2 + R^2 + z^2 + 2\rho R - 4\rho R \sin^2\beta)^{1/2}} \tag{12}$$

Then, by introducing

$$\mu = k^2 = \frac{4\rho R}{q} \text{ where } q = R^2 + \rho^2 + z^2 + 2\rho R \tag{13}$$

where $k = \sqrt{\mu}$ is the modulus of Jacobian elliptic functions (Abramowitz & Stegun, 1964).

According to the textbooks on special functions, the physical restriction in (13) indeed bounds k to the interval [0, 1]. Substituting this into the potential [Eq. (12)] leads to the following expression:

$$V(\rho,z) = k_e \frac{2}{\pi} \frac{Q}{\sqrt{q}} \int_0^{\pi/2} \frac{d\beta}{\sqrt{1-k^2 \sin^2\beta}} \tag{14}$$

The potential depends on the q and k parameters, which in turn depend on (ρ, z) [Eq. (13)].

In this expression, we can recognize the form of the complete elliptic integral of the first kind, often denoted $K(k^2)$, and defined as :

$$K(k^2) = \int_0^{\pi/2} \frac{d\beta}{\sqrt{1-k^2 \sin^2\beta}} \tag{15}$$

This is Legendre's complete elliptic integral of the first kind, which is defined for $0 \leq k \leq 1$, as described in Arfken & Weber (2005). At $k = 0$, $K(0) = \pi/2$, and as k approaches 1, $K(k^2)$ approaches ∞.

For computational purposes, the elliptic integral can be expanded into a power series (Chapman et al., 2022):

$$K(k^2) = \frac{\pi}{2} \sum_{n=0}^{\infty} \left(\frac{(2n)!}{2^{2n}(n!)^2} \right) k^{2n} = \frac{\pi}{2} \sum_{n=0}^{\infty} \left(P_{2n}(0) \right)^2 k^{2n} , \tag{16}$$

where P_n is the Legendre polynomials, which is equivalent to

$$K(k^2) = \frac{\pi}{2} \left(1 + \left(\frac{1}{2} \right)^2 k^2 + \left(\frac{1.3}{2.4} \right)^2 k^4 + \ldots + \left(\frac{(2n-1)!!}{(2n)!!} \right)^2 k^{2n} + \ldots \right) \tag{17}$$

where $(n)!!$ denotes the double factorial. This series offers an efficient method for approximate numerical evaluation of the potential (Narayanan, 2020).

Finally, the **canonical form** of the potential is:

$$V(\rho,z) = k_e \frac{2}{\pi} \frac{Q}{\sqrt{q}} K(k^2) \tag{18}$$

The compact form of Eq. (18) completely describes the potential of a uniformly charged ring and establishes its differentiability everywhere except on the ring itself, as shown in Fig. 2. This property follows from the behaviour of the complete elliptic integral of the first kind, defined in Eq. (15), which increases monotonically from K(0) = π/2 to K(1) $\rightarrow \infty$ (Abramowitz & Stegun, 1964; Arfken & Weber, 2005; Gradshteyn & Ryzhik, 2007), as illustrated in Fig. 3. Accordingly, the potential in Eq. (18) is differentiable only within this domain of definition. The singularity likewise propagates to the electric field of the ring of charge.
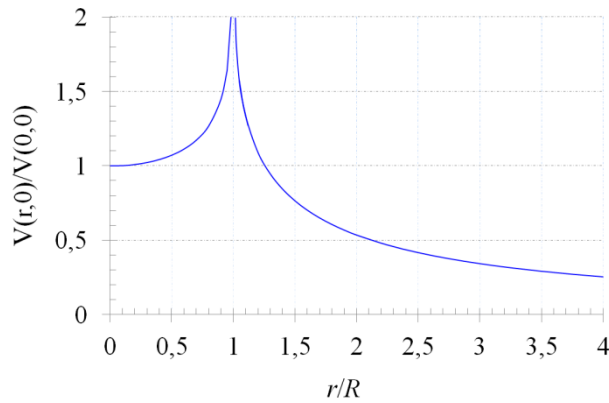
ICTELS
www.ictels.net

International Conference on Technology, Engineering, and Life Sciences
May 16-19, 2025   Rome, Italy

iSTES
www.istes.org

Figure 2. Electric potential in the plane of a uniformly charged ring as a function of the relative radius $a = r/R$. As we see, the potential vanishes at the center ($a = 0$) and diverges as $a \to 1$.

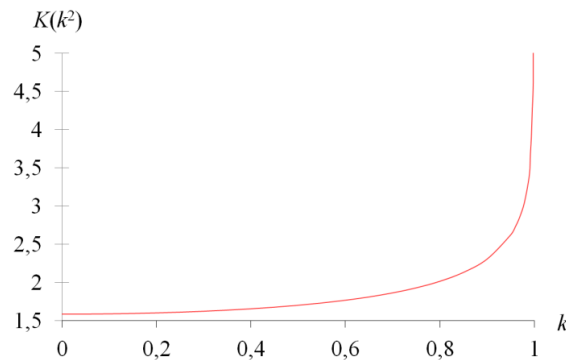**Figure 3**. Complete elliptic integral of the first kind $K(k^2)$ as a function of the modulus k.

Electric Field Derived from the Potential

According to the symmetry study, the electric field vector of a uniformly charged ring should have two components: a radial component and an axial component; the azimuthal component should be zero. Furthermore, the invariance study shows that the electric field vector is independent of the azimuthal angle φ, depending only on the cylindrical coordinates ρ and z. Accordingly, the implicit expression of the electric field vector in cylindrical coordinates should have the following general form:

$$\mathbf{E}(\rho, z) = E_\rho(\rho, z)\, \boldsymbol{u}_\rho + E_z(\rho, z)\, \boldsymbol{u}_z \tag{19}$$

According to Maxwell's second equation of the electrostatic field at a point P in space, curl $\mathbf{E} = \mathbf{0}$.
Thus, an electric field vector can be derived from a scalar electric potential field by applying the gradient operator to the latter, $\mathbf{E} = -\mathbf{grad}\,V$. Otherwise,

$$\mathbf{E}(\rho, z) = -\nabla V(\rho, z) \tag{20}$$

Applying the gradient operator vector [**Eq. (20)**] in cylindrical coordinates to the potential results in:

$$\mathbf{E}(\rho, z) = -\nabla V(\rho, z) = -\left(\frac{\partial}{\partial \rho} \boldsymbol{u}_\rho + \frac{\partial}{\partial z} \boldsymbol{u}_z \right) V(\rho, z) \tag{21}$$

The electric field component along the unit vector $\boldsymbol{u}_\varphi$ is zero, *i.e.*, $E_\varphi = 0$, because the electric potential does not depend on the azimuthal angle φ by invariance study. However, determining the field components in Eq. (21) requires deriving the complete elliptic integral of the first kind, $K(k^2)$, into the expression (18). This involves deriving the function (15) as follows:

$$\frac{\partial K(k^2)}{\partial k} = \int_0^{\pi/2} \frac{\partial}{\partial k} \left(\frac{1}{\sqrt{1 - k^2 \sin^2 \beta}} d\beta \right) \tag{22}$$

After deriving this, we obtain:

$$\frac{\partial K(k^2)}{\partial k} = \int_0^{\pi/2} \frac{k \sin^2 \beta}{1 - k^2 \sin^2 \beta} \frac{d\beta}{\sqrt{1 - k^2 \sin^2 \beta}} \tag{23}$$

Differentiating $K(k^2)$ with respect to k, we obtain:

$$\frac{\partial K(k^2)}{\partial k} = \frac{E(k^2) - (1 - k^2) K(k^2)}{k(1 - k^2)} \tag{24}$$

Here, $K(k^2)$ and $E(k^2)$ are the complete elliptic integrals of the first and second kinds, respectively.

Axial Component Calculation

In order to derive the axial component of the electric field, as it appears in Eq. (19), from the potential gradient given in Eq. (21), the following partial derivatives must be evaluated:

$$\frac{\partial q}{\partial z} = 2z \tag{25a}$$

$$\frac{\partial \sqrt{q}}{\partial z} = \frac{z}{\sqrt{q}} \tag{25b}$$

$$\frac{\partial K(k^2)}{\partial z} = \frac{\partial K(k^2)}{\partial k} \frac{\partial k}{\partial z} \tag{25c}$$

$$\frac{\partial k}{\partial z} = 2(\rho R)^{1/2}(2z)\left(-\frac{1}{2}\right)(q)^{-3/2} = -2z(\rho R)^{1/2}(q)^{-3/2} = -\frac{zk}{q} = -\frac{zk^3}{4\rho R} \tag{25d}$$

$$\frac{\partial V(\rho,z)}{\partial z} = k_e Q \frac{2}{\pi} \frac{\frac{\partial K(k^2)}{\partial k}\frac{\partial k}{\partial z}\sqrt{q} - K(k^2)\frac{\partial \sqrt{q}}{\partial z}}{q} \tag{26}$$

Substituting derivatives (23) and (25a–d) into (26) and performing the required simplifications, we obtain:

$$\frac{\partial V(\rho,z)}{\partial z} = -k_e \frac{Q}{\pi}\frac{2}{q^{3/2}}z\int_0^{\pi/2}\frac{1}{1-k^2 sin^2\beta}\frac{d\beta}{\sqrt{1-k^2 sin^2\beta}} \tag{27}$$

This result corresponds to the axial component E_z of the electric field vector in Eq. (21), except it has an extra negative sign. As the field vector is defined as the negative gradient of the potential, this extra sign cancels out when substituted into the gradient operator of Eq. (21). Thus, the axial component is given by:

$$E_z(\rho,z) = -\frac{\partial V(\rho,z)}{\partial z}$$
$$= k_e \frac{Q}{\pi}\frac{2}{q^{3/2}}z\int_0^{\pi/2}\frac{1}{1-k^2 sin^2\beta}\frac{d\beta}{\sqrt{1-k^2 sin^2\beta}} \tag{28}$$

At this stage, one option is to proceed numerically by evaluating expression (28) directly using computational methods. Alternatively, further analytical manipulation allows for the derivation of a more compact form. To this end, we proceed as follows.

The complete elliptic integral of the third kind is defined as (Good, 2001; Noh, 2017):

$$\Pi(n|m) = \int_0^{\pi/2}\frac{1}{1-n\,sin^2\beta}\frac{d\beta}{\sqrt{1-m\,sin^2\beta}} \tag{29}$$

where n denotes the elliptic characteristic and m the elliptic modulus (Weisstein, 2025). For real values of m, it is always possible to arrange $0 \square m \square 1$ (Abramowitz & Stegun, 1964) since m = k2.

A noteworthy special case occurs when both the characteristic and the modulus are equal (*i.e.*, $n = m = k^2$). In this case, integral (29) reduces to:

$$\Pi\left(k^2 \middle| k^2\right) = \int_0^{\pi/2}\frac{1}{1-k^2 sin^2\beta}\frac{d\beta}{\sqrt{1-k^2 sin^2\beta}} \tag{30}$$

Examining the axial component in Eq. (28) shows that it encompasses the special case of the complete elliptic integral of the third kind with $n = m = k^2$. Therefore, the axial component of the electric field can be expressed as follows:

$$E_z(\rho,z) = k_e \frac{Q}{\pi}\frac{2}{q^{3/2}}z\,\Pi(k^2|k^2) \tag{31}$$

According to Arfken & Weber (2005) & Weisstein (2025), when k2 = 1 the function diverges, whereas for $0 \leq k2 \leq 1$ it remains finite but increases with k□. In particular, □(k2□k2) diverges for k2=1 and satisfies □(0□0) = □/2, as illustrated in Fig. 4. Furthermore, there exists a functional relationship between □(k2□k2) and the complete elliptic integral of the second kind, E(k2), given by (Abramowitz & Stegun, 1964; Gradshteyn & Ryzhik, 2007; Weisstein, 2025):

$$\Pi\left(k^2 \middle| k^2 \right) = \frac{E(k^2)}{1 - k^2} \tag{32}$$

where

$$E(k^2) = \int_0^{\pi/2} \sqrt{1 - k^2 \sin^2\beta} \, d\beta \tag{33}$$

$E(k^2)$ can also be represented as a power series (Carleton, 2022; Chapman et al., 2022):

$$E(k^2) = \frac{\pi}{2} \sum_{n=0}^{\infty} \left(\frac{(2n)!}{2^{2n}(n!)^2} \right)^2 \frac{k^{2n}}{1 - 2n}, \tag{34}$$
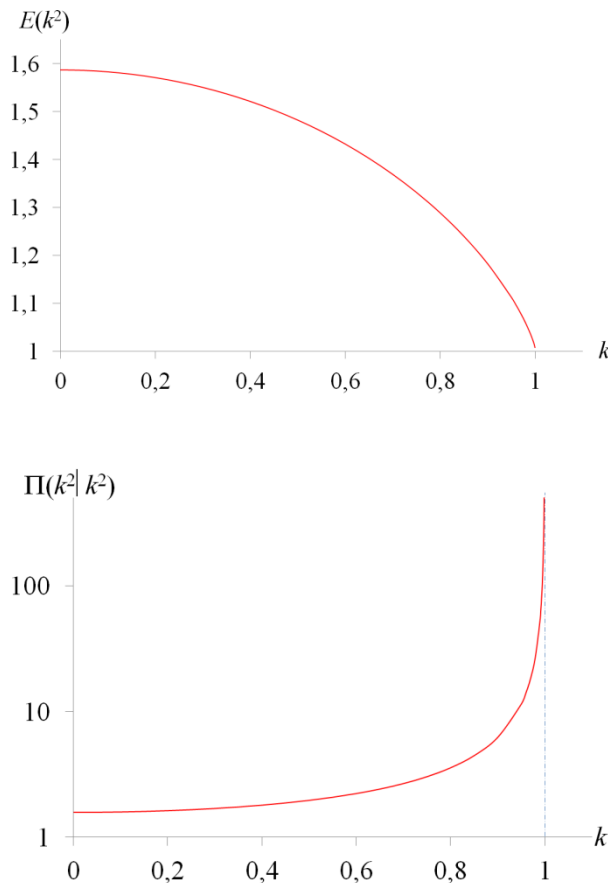

Figure 4. Complete elliptic integrals of the second and third kinds as a function of the modulus *k*.

As we see, □(k²□k²) → ∞ when *k* → 1.

which is equivalent to

$$E(k^2) = \frac{\pi}{2}\left(1 - \left(\frac{1}{2}\right)^2 \frac{k^2}{1} - \left(\frac{1.3}{2.4}\right)^2 \frac{k^4}{3} - \dots - \left(\frac{(2n-1)!!}{(2n)!!}\right)^2 \frac{k^{2n}}{2n-1} - \dots\right) \tag{35}$$

Boundary conditions for this function are well established: $E(0) = \Box/2$ and $E(1) = 1$. For $k^2=0$, it follows that $\Box(k^2\Box k^2) = E(0) = \Box/2$, in agreement with **Fig**. 3. Conversely, for $k^2 = 1$, the denominator in (32) vanishes, leading to divergence and hence a singularity. Nevertheless, relation (32) remains valid and provides a means of calculating $\Box(k^2 \Box k^2)$ in terms of $E(k^2)$.

By substituting the expression of $\Box(k^2 \Box k^2)$ from (32) into (31), the axial component of the electric field vector can be recast into the more compact form:

$$E_z(\rho, z) = k_e \frac{Q}{\pi} \frac{2}{(1-k^2)q^{3/2}} z E(k^2) \tag{36}$$

This final expression corresponds to the axial component E_z originally predicted by the implicit relation (19).

As noted by Mandre (2007), the same result may alternatively be obtained by employing the differential equation for the complete elliptic integral of the first kind, as defined in (24), into (26) in place of (23).

1.1. Radial Component Calculation

The derivation of the axial component E_z can be extended naturally to the radial component E_ρ. In particular, E_ρ can also likewise be expressed in terms of standard elliptic integrals. To obtain the explicit form of the radial field component given in Eq. (19) from the gradient of the potential in Eq. (21), the following partial derivatives must first be evaluated:

$$\frac{\partial q}{\partial \rho} = 2(\rho + R) \tag{37a}$$

$$\frac{\partial \sqrt{q}}{\partial \rho} = \frac{\rho + R}{\sqrt{q}} \tag{37b}$$

$$\frac{\partial K(k^2)}{\partial \rho} = \frac{\partial K(k^2)}{\partial k} \frac{\partial k}{\partial \rho} \tag{37c}$$

$$\frac{\partial k}{\partial \rho} = 4R\left(\frac{1}{2}\right)(4\rho R)^{-1/2}q^{-1/2} + (4\rho R)^{1/2}\left(-\frac{1}{2}\right)q^{-3/2}(2R+2\rho)$$

$$= 2R(4\rho R)^{-1/2}\frac{k}{2(\rho R)^{1/2}} - (4\rho R)^{1/2}\left(\frac{1}{2}\right)\frac{k^3}{8\rho R(\rho R)^{1/2}}(2R+2\rho) \tag{37d}$$

$$= \frac{k}{2\rho} - \frac{k^3}{8\rho R}(2R+2\rho)$$

$$= \frac{k}{2\rho} - \frac{k^3}{4\rho} - \frac{k^3}{4R}$$

Differentiating Eq. (18) with respect to ρ:

$$\frac{\partial V(\rho,z)}{\partial \rho} = k_e Q \frac{2}{\pi} \frac{\dfrac{\partial K(k^2)}{\partial k}\dfrac{\partial k}{\partial \rho}\sqrt{q} - K(k^2)\dfrac{\partial \sqrt{q}}{\partial \rho}}{q} \tag{38}$$

Substituting Eqs. (23) and (37a–d) into Eq. (38), followed by algebraic simplification, yields

$$\frac{\partial V(\rho,z)}{\partial \rho} = -k_e \frac{Q}{\pi}\frac{2}{q^{3/2}}\left[\rho\int_0^{\pi/2}\frac{1}{(1-k^2\sin^2\beta)^{3/2}}d\beta + R\int_0^{\pi/2}\frac{1-2\sin^2\beta}{(1-k^2\sin^2\beta)^{3/2}}d\beta\right] \tag{39}$$

From Eq. (21), the explicit form of the radial component of the field is then,

$$E_\rho(\rho,z) = -\frac{\partial V(\rho,z)}{\partial \rho}$$

$$= k_e \frac{Q}{\pi}\frac{2}{q^{3/2}}\left\{\rho\int_0^{\pi/2}\frac{1}{(1-k^2\sin^2\beta)^{3/2}}d\beta + R\int_0^{\pi/2}\frac{1-2\sin^2\beta}{(1-k^2\sin^2\beta)^{3/2}}d\beta\right\} \tag{40}$$

Equation (40) shows that $E_\square$ involves two elliptic integrals. The first is the complete elliptic integral of the third kind with parameters $n = k^2$ and $m = k^2$, while the second contains the factor $(1 \square \square 2\sin^2\square)$ in the numerator, making its reduction less straightforward. To simplify, we decompose the integral as

$$E_\rho(\rho,z) = k_e \frac{Q}{\pi}\frac{2}{q^{3/2}}\left\{\rho\int_0^{\pi/2}\frac{d\beta}{(1-k^2\sin^2\beta)^{3/2}} + R\int_0^{\pi/2}\frac{d\beta}{(1-k^2\sin^2\beta)^{3/2}} + \int_0^{\pi/2}\frac{-2R\sin^2\beta}{(1-k^2\sin^2\beta)^{3/2}}d\beta\right\} \tag{41}$$

and, by multiplying the numerator and denominator appropriately, rewrite it as

$$E_\rho(\rho,z) = k_e \frac{Q}{\pi}\frac{2}{q^{3/2}}\left\{(\rho+R)\int_0^{\pi/2}\frac{d\beta}{(1-k^2\sin^2\beta)^{3/2}} + \frac{1}{\rho}\int_0^{\pi/2}\frac{-2R\rho\sin^2\beta}{(1-k^2\sin^2\beta)^{3/2}}d\beta\right\} \tag{42}$$

At this stage, auxiliary terms are introduced and rearranged to give

$$E_\rho(\rho,z) = k_e \frac{Q}{\pi} \frac{2}{q^{3/2}} \left\{ (\rho + R) \int_0^{\pi/2} \frac{d\beta}{(1-k^2 sin^2\beta)^{3/2}} + \frac{1}{\rho} \int_0^{\pi/2} \frac{\frac{R^2}{2} - \frac{R^2}{2} - 2R\rho \, sin^2\beta + \frac{\rho^2}{2} - \frac{\rho^2}{2} + \frac{z^2}{2} - \frac{z^2}{2}}{(1-k^2 sin^2\beta)^{3/2}} d\beta \right\}$$

(43)

Rearranging, the radial component yields

$$E_\rho(\rho,z) = k_e \frac{Q}{\pi} \frac{2}{q^{3/2}} \left\{ \begin{array}{l} (\rho + R) \int_0^{\pi/2} \frac{d\beta}{(1-k^2 sin^2\beta)^{3/2}} \\ + \frac{1}{\rho} \int_0^{\pi/2} \frac{\frac{1}{2}((R+\rho)^2 + z^2) - 2R\rho \, sin^2\beta - \frac{1}{2}(R^2 + \rho^2 + z^2 + 2R\rho)}{(1-k^2 sin^2\beta)^{3/2}} d\beta \end{array} \right\}$$

(44)

Using relation (13), which rewrites $q = \Box(\Box + R)^2 + z^2\Box$ by $q = 4\Box R/k^2$, we obtain

$$E_\rho(\rho,z) = k_e \frac{Q}{\pi} \frac{2}{q^{3/2}} \left\{ \begin{array}{l} (\rho + R) \int_0^{\pi/2} \frac{d\beta}{(1-k^2 sin^2\beta)^{3/2}} \\ + \frac{1}{\rho} \int_0^{\pi/2} \frac{\frac{2\rho R}{k^2}(1-k^2 sin^2\beta)}{(1-k^2 sin^2\beta)^{3/2}} d\beta - \frac{1}{\rho} \int_0^{\pi/2} \frac{\frac{1}{2}\frac{4\rho R}{k^2}}{(1-k^2 sin^2\beta)^{3/2}} d\beta \end{array} \right\}$$

(45)

Further simplification leads to a more compact expression,

$$E_\rho(\rho,z) = k_e \frac{Q}{\pi} \frac{2}{q^{3/2}} \left\{ (\rho + R) \int_0^{\pi/2} \frac{d\beta}{(1-k^2 sin^2\beta)^{3/2}} + \frac{2R}{k^2} \int_0^{\pi/2} \frac{d\beta}{(1-k^2 sin^2\beta)^{1/2}} - \frac{2R}{k^2} \int_0^{\pi/2} \frac{d\beta}{(1-k^2 sin^2\beta)^{3/2}} \right\}$$

(46)

Here, the middle term corresponds to the complete elliptic integral of the first kind $K(k^2)$ [Eq. (15)], while the other two are special cases of the complete elliptic integral of the third kind $\Box(n\Box m)$ with $n = k^2$ and $m = k^2$ [Eq. (30)]. Substituting these forms, the radial field reduces to

$$E_\rho(\rho,z) = k_e \frac{Q}{\pi} \frac{2}{q^{3/2}} \left\{ (\rho + R)\Pi\left(k^2 \Big| k^2 \right) + \frac{2R}{k^2} K(k^2) - \frac{2R}{k^2} \Pi\left(k^2 \Big| k^2 \right) \right\}$$

(47)

Then, using relation (32) again, we get,

$$E_\rho(\rho,z) = k_e \frac{Q}{\pi} \frac{2}{q^{3/2}} \left\{ (\rho + R)\frac{E(k^2)}{1-k^2} + \frac{2R}{k^2} K(k^2) - \frac{2R}{k^2}\frac{E(k^2)}{1-k^2} \right\}$$

(48)

Finally, upon reordering, we obtain

$$E_\rho(\rho,z) = k_e Q \frac{2}{\pi k^2 (1-k^2) q^{3/2}} \left\{ 2R(1-k^2)K(k^2) - (2R - k^2(\rho+R))E(k^2) \right\} \tag{49}$$

which coincides with the implicit form of Eq. (19). As noted by Mandre (2007), the same result may be derived directly from the differential equation for the complete elliptic integral of the first kind [Eq. (24)], rather than Eq. (23), in the differentiation step (38).

Results

We thus arrive at explicit expressions for the electric field components corresponding to Eqs. (19) and (21). The radial and axial components of the field due to a uniformly charged ring at an arbitrary point in space are given by the following equations:

$$E_\rho(\rho,z) = k_e Q \frac{2}{\pi \mu(1-\mu) q^{3/2}} \left(2R(1-\mu)K(\mu) - (2R - \mu(\rho+R))E(\mu) \right) \tag{50a}$$

$$E_z(\rho,z) = k_e \frac{Q}{\pi} \frac{2}{(1-\mu) q^{3/2}} z\, E(\mu) \tag{50b}$$

where $q = \rho^2 + R^2 + z^2 + 2\rho R$, $\mu = k^2 = \dfrac{4\rho R}{q}$, and $K(\mu)$ and $E(\mu)$ denote the complete elliptic integrals of the first and second kinds, respectively.

Equations (50a–b) represent the most compact form of the field components for this configuration.
As illustrated in **Fig**s. 3 and 4, the point $k^2 = 1$ is a singularity for both the complete elliptic integrals of the first and third kinds. Consequently, the radial component diverges as $k \to 1$.

Numerical evaluation of the elliptic integrals in Eqs. (50a–b) can be performed using computational packages such as MATLAB, MATHEMATICA, or ALGLIB Elliptic Integral subroutines for C++ / Java / Python, etc.

In-Plane and On-Axis Field of the Ring of Charge
In-Plane

The electric field in the plane of the ring of charge can be expressed in terms of standard elliptic integrals using Eq. (50a), while Eq. (50b) vanishes because $z = 0$ (Saâd, 2025). Consequently,

$$E_r(r,0) = k_e \frac{Q}{\pi} \frac{2}{q^{3/2}} \frac{1}{\mu} \frac{1}{(1-\mu)} \left\{ 2R(1-\mu)K(\mu) - (2R - \mu(r+R))E(\mu) \right\} \tag{51}$$

where

$$q = R^2 + r^2 + 2rR = R^2(1 + 2a + a^2) = R^2(1+a)^2 \tag{51a}$$

and

$$\mu = k^2 = \frac{4rR}{q} = \frac{4rR}{(R+r)^2} = \frac{4a}{1 + 2a + a^2} \tag{51b}$$

As $Q = 2\pi R\lambda$, function (51) simplifies to

$$E_r(r,0) = k_e \frac{\lambda}{R} \frac{(1+a)}{a} \frac{1}{(1-a)^2} \left\{ 2(1-\mu)K(\mu) - (2 - \mu(1+a))E(\mu) \right\} \tag{52}$$

Table 1 presents the field values, expressed as $k_e\lambda/R$ in IS units, given for various concentric circles with relative radii $a \in [0, 1[\cup]1, 4]$. The field in the plane of the ring diverges at $r/R = 1$, indicating a singularity as predicted by the curves of the potential of a uniform ring of charge shown in **Fig**. 2.

Figure 5 shows the electric field amplitude as a function of the ratio $a = r/R$. The field vanishes at the center of the ring and diverges at $a = 1$, corresponding to a singular point at the ring's edge. As point P approaches this edge, the field tends to infinity, reflecting the behavior of the elliptic integrals in **Fig**. (3). Nevertheless, for a real conductor with finite volume, the field inside the ring would be zero, since the ring's surface is closed and any excess charge resides on the surface.

The minus sign (−) in Table 1 and **Fig**. 5 indicates that the electric field vector points in the opposite direction to the unit vector $\boldsymbol{u}_\rho$, since $\lambda > 0$. Outside the ring, the vector aligns with $\boldsymbol{u}_\rho$.

On a given field line, the orientation of the electric field vector is opposite inside the ring and along the same direction outside it (Zypman, 2006).

Table 1. In-Plane Field of a Uniformly Charged Ring as a Function of Relative Radius.

$a = r/R$	$E_r (\times k_e\lambda/R)$	$a = r/R$	$E_r (\times k_e\lambda/R)$
0	0,000	1,001	46,188
0,1	-0,318	1,1	22,005
0,2	-0,658	1,2	11,310
0,3	-1,048	1,3	7,551
0,4	-1,528	1,4	5,606
0,5	-2,167	1,5	4,410
0,6	-3,100	1,6	3,599

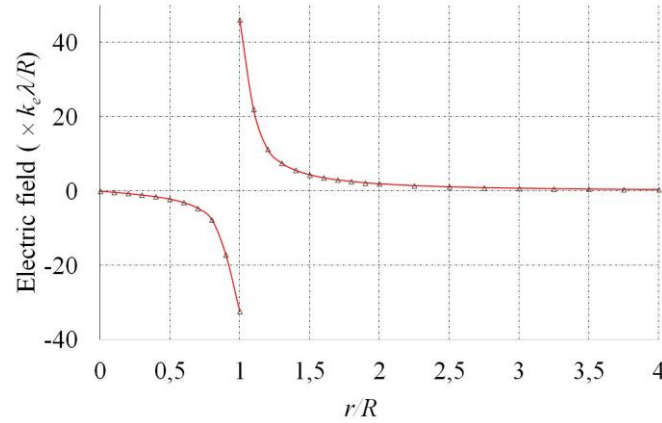|			
0,7	-4,641	1,7	3,015
0,8	-7,744	1,8	2,574
0,9	-17,184	1,9	2,231
0,999	-32,368	2	1,957

Figure 5. Electric field amplitude in the plane of a uniformly charged ring as a function of the relative radius $a=r/R$. The field vanishes at the center ($a=0$) and diverges as $a \rightarrow 1$.

On-Axis

Due to the symmetry, only the axial component of the field remains. Therefore, Eqs. (50a–b) reduces to

$$E_z(\rho, z) = k_e \frac{Q}{\pi} \frac{2}{(1-\mu)q^{3/2}} z \, E(\mu) \tag{53}$$

The field along the z axis of the ring corresponds to $\theta = 0$, as shown in **Fig**. 1, which places the point P on the z axis, i.e., $r = z$. Since P$\in z$ axis, here, the coordinate z represents the distance from the center O of the ring to the point P on the z axis. It should be noted that the expression of the electric field on the axis of the ring can be derived from the components (50a–b) of the field vector (Saâd, 2025). In effect, to obtain this result, one must substitute the parameters ρ, z, q, and k with their corresponding values for $\theta = 0$: $\rho = 0$, $q = (R^2 + z^2)$ where $z \equiv r$, $k = 0$ into Eqs. (50a–b). After simplification, Eq. (53) exactly takes the following form:

$$\mathbf{E}(z) = k_e \frac{Q z}{(R^2 + z^2)^{3/2}} \boldsymbol{u}_z \tag{54}$$

It is worth mentioning that this special case is the one most frequently presented in textbooks and online resources on Electrostatics; hence, it is already familiar to many undergraduate students.

However, when the point P is located at the center ($z = 0$), the electric field vanishes ($\mathbf{E} = \mathbf{0}$). In contrast, for $z \gg R$, Eq. (54) reduces to the following approximation:

$$\mathbf{E}(z) = k_e \frac{Q z}{(R^2 + z^2)^{3/2}} \boldsymbol{u}_z \approx k_e \frac{Q}{z^2} \boldsymbol{u}_z = k_e \frac{Q}{r^2} \boldsymbol{u}_z \tag{55}$$

Usefulness of Charged Rings

The charged ring is more than a pedagogical model; it is a fundamental element whose non-uniform electric field governs particle dynamics in advanced scientific instruments. The obtained results show that the field is not uniform in three-dimensional space. A critical property of such electric fields is that the motion of initially static charged particles follows trajectories tangent to the field lines at every point. This principle is leveraged in devices designed to control and manipulate charged particles.

A primary application is in electrostatic ion traps, such as the electrostatic ion storage ring and the electrostatic ion beam trap (Andersen et al., 2004; Gumberidze et al., 2009). In these devices, configurations of electrodes, which can be conceptually modeled as segments of charged rings, create a specific non-uniform field that provides transverse focusing (confinement) and longitudinal guidance for ion beams, enabling experiments in atomic and molecular physics over extended periods. Similarly, the field geometry is exploited in mass spectrometers (Zypman, 2006), where charged rings, or their electrode equivalents, are used to focus ion beams. The precise control over the particle trajectories afforded by the ring's field is essential for achieving high resolution in separating ions by their mass-to-charge ratio. This principle extends to electronic optics (Goyal, 2024), where ring-like electrodes act as electrostatic lenses to focus particle beams.

On a much larger scale, the concept finds application in nuclear fusion research. In devices like Tokamak Fusion Reactors, the magnetic fields used to confine hot plasma are generated by currents flowing in toroidal coils, which can be modeled as a series of charged rings. The electromagnetic forces derived from these configurations are critical for containing the plasma and achieving the conditions necessary for fusion.
However, applying this model to real-world devices presents significant challenges. The shape and size of rings vary greatly between applications. A major contemporary challenge lies at the microscopic scale, where the charge and size of nanoscopic rings must be measured using techniques like atomic force microscopy (Gordon et al., 2024). A central problem in this field is the accurate calculation of tip-sample forces (Eisenberg & Zypman, 2019; Lazarev & Zypman, 2017), which directly depends on precisely modeling the electric field of the charged nanostructure, a challenge highlighted by Gordon et al. (2024) for measuring ring charge via scanning force microscopy.

Beyond these established applications, the physics of charged rings inspires research into diverse topics, including the dynamics of particle-beam weapons (Zhou & Qian, 2014) and the fundamental oscillations of a pair of charged rings (Sarafian, 2020). Thus, from guiding particles in traps to posing challenges in nanoscale metrology, the charged ring remains an endless source of relevant research topics in modern physics.

Conclusion

This study has presented a rigorous derivation of the off-axis electric potential and field of a uniformly charged

ring. Direct integration of Coulomb's law yielded the potential in terms of the complete elliptic integral of the first kind, while applying the gradient provided the electric field vector more efficiently than direct component integration. The field was shown to contain radial and axial contributions, with the azimuthal component vanishing by symmetry, and was expressed compactly using elliptic integrals.

Beyond its analytical value, the model offers direct relevance to applied systems. The thin-ring formulation provides a foundation for modeling the non-uniform fields that govern charged particle dynamics in devices such as mass spectrometers and electrostatic ion traps. Through superposition, it also serves as a building block for more complex charge distributions, with accuracy controlled by discretization. Extensions to Cartesian and spherical coordinates would further broaden its applicability to problems with differing symmetries.

In summary, the methodology developed here delivers a consistent and computationally efficient platform for theoretical development and applied modeling in electrostatics, supporting both the analysis and optimization of advanced charged-particle technologies.

Acknowledgments

References

Abramowitz, M., Stegun, I. A. (1964). *Handbook of Mathematical Functions: With Formulas, Graphs, and Mathematical Tables*. Dover Publications.

Andersen, L. H., Heber, O., Zajfman, D. (2004). Physics with electrostatic rings and traps. *Journal of Physics B: Atomic, Molecular and Optical Physics*, *37*(11), R57-R88. doi 10.1088/0953-4075/37/11/R01

Arfken, G. B., Weber, H. J. (2005). *Mathematical Methods For Physicists*. Elsevier Academic Press.

Bochko, V. Y., Silagadze, Z. K. (2020). On the electrostatic potential and electric field of a uniformly charged disk. *European Journal of Physics*, *41*(4), 045201. https://doi.org/10.1088/1361-6404/ab87aa

Boridy, I. (2005). *Electromagnétisme : Théorie et Applications*. Presse de l'Université du Québec.

Carleton, D. (2022). Undergraduate Thesis Current Loop Off-Axis Field Approximations. Retrieved March 08, 2025, from https://summit.sfu.ca/_flysystem/fedora/2023-04/DanielCarletonFinalUGThesisEngSci2022.pdf

Chapman, G. H., Carleton, D. E., Sahota, D. G. (2022). Current Loop Off Axis Field Approximations With Excellent Accuracy and Low Computational Cost. *IEEE Transactions on Magnetics*, *58*(*8*), 3149010 https://ieeexplore.ieee.org/document/9703286

Ciftja, O. (2023). Stored electrostatic energy of a uniformly charged annulus. *Journal of Electrostatics*, *122*, 103794. https://doi.org/10.1016/j.elstat.2023.103794

Ciftja, O., Babineaux, A., Hafeez, N. (2009). The electrostatic potential of a uniformly charged ring. *European Journal of Physics*, *30*(3), 623-627. https://iopscience.iop.org/article/10.1088/0143-0807/30/3/019

Ciftja, O., Bentley, C. L. (2024). Electrostatic potential of a uniformly charged annulus. *European Journal of Physics*, *45*(3), 035201. https://iopscience.iop.org/article/10.1088/1361-6404/ad2cf6

Ulaby, F. T. (2007). *Fundamentals of Applied Electromagnetics*. Prentice Hall.

Eisenberg, Y., Zypman, F. R. (2019). Ring of charge probed with AFM dielectric tip. *Journal of Electrostatics*, *97*, 95-100. https://doi.org/10.1016/j.elstat.2019.01.002

Escalante, F. (2021). Electrostatic potential and electric field in the z axis of a non-centered circular charged ring. *European Journal of Physics*, *42*(6) 65703. https://iopscience.iop.org/article/10.1088/1361-6404/ac221c

Good, R. H. (2001). Elliptic integrals, the forgotten functions. *European Journal of Physics*, *22*(2), 119-126. https://iopscience.iop.org/article/10.1088/0143-0807/22/2/303

Gordon, M., Goykadosh, B., Magendzo, Y., Zypman, F. (2024) Theory for measuring electric charge density of a ring from scanning force microscopy. *AIP Advances, 14*(10), 105211. https://doi.org/10.1063/5.0221217

Goyal, A. (2024, August 22). Charged Ring as Electrostatic Lens. YouTube. Retrieved March 08, 2024, from https://youtu.be/WlpmYl_QVRU

Gradshteyn, I. S., Ryzhik, I. M. (2007). *Table of integrals, series, and products*. (Scripta Technica, Inc, Trans.). Elsevier Inc. (A. Jeffrey, Ed.; D. Zwillinger, Ed. ; V. Moll, Sci. Ed.).

Gumberidze, A., Attia, D., Szabo, C. I., Indelicato, P., Vallette, A., Carmo, S. (2009). Trapping of highly charged ions with an electrostatic ion trap. *Journal of Physics: Conference Series*, *163*, 163 012110. https://iopscience.iop.org/article/10.1088/1742-6596/163/1/012110

Lazarev, D., Zypman, F. R. (2017). Charge and size of a ring in an electrolyte with atomic force microscopy. *Journal of Electrostatics*, *87*, 243-250. https://doi.org/10.1016/j.elstat.2017.05.004

Mandre, I. (2007, July 1). Ephi - the simple physics simulator. Indrek's Hom*epage*.

Retrieved March 18, 2024, from http://www.mare.ee/indrek/ephi/

Martín-Luna, P., Gimeno, B., Esperante, D. (2023). Comment on 'On the electrostatic potential and electric field of a uniformly charged disk'. *European Journal of Physics*, *44*(6), 068003. https://iopscience.iop.org/article/10.1088/1361-6404/acf81c

Narayanan, Vivek (2020). Electric potential off axis of charged ring. YouTube. Retrieved July 15, 2023, from https://youtu.be/X1WMeblOi_o

Noh, H. (2017). Electrostatic Potential of a Charged Ring: Applications to Elliptic Integral Identities. *Journal of the Korean Physical Society*, *71*, 37-41. https://doi.org/10.3938/jkps.71.37

Pérez, J.-P., Carles, R., Fleckinger, R. (2002). *Électromagnétisme, Fondements et applications*. Dunod. https://www.calameo.com/read/0046004893b8f742492ce

Plonus, M. A. (1978). *Applied Electromagnetics*. New York: McGraw-Hill, Inc.

Sarafian, H. (2020). Nonlinear Oscillations of a Pair of Charged Rings. *American Journal of Computational Mathematics*, *10*(4) 571-577. DOI: 10.4236/ajcm.2020.104032

Sagaydak, A. E., Silagadze, Z. K. (2024). Electrostatic potential of a uniformly charged disk through Green's theorem. *European Journal of Physics*, *46*(1), 1-10. https://doi.org/10.1088/1361-6404/ad9ae8

Serway, R. A., Jewett, J. W. (2014). *Physics for Scientists and Engineers with Modern Physics*.

Brooks/Cole Cengage Learning, Boston.

Ulaby, F. T. (2015). *Fundamentals of Applied Electromagnetics*. Umberto Ravaioli Pearson

Weisstein, E. W. (2025, March 5). Elliptic Integ*rals*. Wolfram Research Inc.

Retrieved March 16, 2025, from https://mathworld.wolfram.com/

Wissner-Gross, Zachary (2012, January 9). Electric field inside a charged ring. YouTube.

Retrieved July 15, 2023, from https://youtu.be/BF3wEV4tWq8

Young, H. D., Freedman, R. A. (2012). *Sears and Zemansky's University Physics: with modern physics*. Addison-Wesley Pearson Education Inc.

Zhou, C., Qian, W. (2014). Particle-beam weapons system. *IEEE International Conference on Control Science and Systems Engineering*, Yantai, China, 81-84. doi:10.1109/CCSSE.2014.7224513

Zypman, F. R. (2006). Off-axis electric field of a ring of charge. *American Journal of Physics, 74*(4), 295-300. https://doi.org/10.1119/1.2149869

Applying Students' Learning Styles to Optimise Studies

Olga Ovtšarenko

Vilnius Gediminas Technical University, Lithuania, TTK University of Applied Sciences Tallinn, Estonia,

https://orcid.org/0000-0003-3195-4280

Patriks Morevs

Riga Technical University, EKA University of Applied Sciences, Latvia,

https://orcid.org/0000-0003-0274-2860

Abstract: Learning style is one of the individual variables that influence learning. Understanding and utilising students' learning styles can help design compelling educational experiences. This article examines the validity of learning style theories to optimise learning strategies and improve student performance. Drawing on models such as VARK (visual, auditory, reading/writing, kinesthetic) and Kolb's experiential learning theory, the article analyses experimental data obtained from a survey of students participating in the Erasmus Blended Intensive Programme. The study of students' learning style changes during individual and group learning provided interesting results for possible use in developing teaching materials, both for independent student work and for organising specialised intensive training, taking into account individual learning styles to improve engagement, retention, and comprehension. The analysis of existing research provided different approaches to using learning styles to enhance learning effectiveness. By considering different perspectives on the validity of learning styles, the article highlights practical strategies that teachers and students can use to create a more personalised and effective learning environment.

Keywords: Learning Styles, Learning Management, Attributes

Introduction

Learning style, as an individual cognitive parameter, constitutes a significant factor influencing how students perceive, process, and assimilate educational material. A clear understanding of one's learning style enables students to leverage their cognitive strengths more effectively, enhancing academic performance and promoting self-regulated learning. For educators, identifying students' learning styles provides an empirical basis for designing differentiated instructional strategies. Personalised teaching recommendations, which incorporate various pedagogical methods and diverse educational resources, have been shown to foster greater engagement, motivation, and achievement among learners. Accordingly, accurately determining students' learning styles

represents a critical prerequisite for developing effective, learner-centred educational practices.

Despite the theoretical importance of learning style identification, the practical application of this parameter within contemporary teaching practices requires careful optimisation of the measurement procedures. Current instruments designed to assess learning styles typically comprise extensive questionnaires, which, while psychometrically robust, present particular challenges. Administering lengthy questionnaires can lead to respondent fatigue, decreased attention, and variability in response quality, undermining the collected data's reliability and validity. Moreover, the time-intensive nature of these instruments may render them impractical for routine use in dynamic classroom settings.

Given these limitations, there is a clear imperative to refine and streamline the procedures for assessing students' learning styles. An optimised measurement approach must balance maintaining high standards of psychometric quality, specifically reliability and validity, and reducing the cognitive and temporal burden placed on respondents. This study is therefore devoted to developing a shortened, yet psychometrically sound, version of existing learning style questionnaires. The objective is to minimise the number of items required to produce an accurate profile of students' learning styles, without compromising the integrity of the assessment. By achieving this goal, the findings of this study aim to contribute to more efficient and practical applications of learning style theory in educational practice, thereby supporting the broader goals of personalisation and inclusivity in contemporary pedagogy.

The article is organised as follows. Section 2 provides an overview and analysis of existing questionnaires to determine learning style. Section 3 explains the concept of developing questionnaires and their comparative analysis. Section 4 presents the results of the general use of the developed questionnaires. Section 5 presents a discussion of the results, and Section 6 contains concluding remarks, limitations of using the method and future research directions.

Literature Review

Students have diverse learning style preferences, necessitating that educators adapt their teaching strategies by incorporating appropriate learning media and instructional methods (Sulistyanto et al., 2019). Various models have been developed to assess learning styles, with questionnaires being one of the primary tools used for classification and instructional adaptation.

Neil Fleming introduced the VARK learning style model in 2006, categorising learners based on their sensory modality preferences: Visual (V), Aural (A), Read/Write (R), and Kinesthetic (K). The VARK inventory utilises a questionnaire to identify an individual's dominant learning style (VARK, 2025). While the model focuses primarily on sensory preferences, it does not account for factors such as personality, motivation, social preferences, or cognitive traits like introversion and extraversion. Fleming emphasised that simply knowing

one's VARK preference is insufficient to improve learning outcomes; learners must actively adjust their study habits, which requires self-awareness and effort.

The automatic detection of learning styles has become an emerging study area, utilising classification techniques that process data from learner interactions within educational systems. Al Qahtani et al. (2018) examined learning styles among undergraduate students and found that most participants preferred multi-modal learning. Their study also identified gender-based differences: males favoured unimodal learning, while females showed an almost equal preference for bimodal and quadrimodal approaches. However, they found no significant difference in learning styles between genders.

Farkas et al. (2016) suggested that learning preferences alone do not correlate with academic performance; instead, factors such as career goals and study time play a more significant role in success. Similarly, Kurian and Gowda (2023) found no significant association between learning styles and assessment scores, possibly due to students' last-minute cramming habits, which hinder their ability to apply VARK-based study strategies effectively.

Lincă and Matei (2024) explored whether students' academic performance is influenced by their learning styles. Their study, conducted among students in educational sciences, utilised a questionnaire-based approach and found significant differences in academic performance among students with auditory, visual, and kinesthetic learning styles and variations based on the students' year of study. These findings suggest that learning style assessments can help tailor educational methods to improve outcomes.

In the study by Kurian and Gowda (2023), no significant association was found between assessment scores and learning style. This might be due to an irregular approach to academics, where students often learn most of the syllabus on the day before the test and, consequently, cannot utilise effective methods that align with their VARK preference.

Since the traditional approach of filling out special psychological questionnaires has several drawbacks (the additional time that students need to spend to fill out the questionnaire, problems with the accuracy of their answers), automatic methods based on the study of students' observed behavior in the learning environment have been proposed (Bernard et al., 2022). No study identifies learning styles using student data from different curricula or disciplines.

Recent research has explored machine learning and regression analysis as alternatives to traditional questionnaires for detecting learning styles. Altamimi et al. (2022) proposed using regression analysis to predict learning styles, introducing a probabilistic approach to account for students' preferences. Their study demonstrated that regression techniques can effectively identify learning styles, offering a more flexible alternative to rigid classification models.

Ayyoub and Al-Kadi (2024) introduced a semi-supervised machine learning approach that utilises data mining techniques to detect students' learning styles based on the Felder-Silverman model. Their study demonstrated that semi-supervised classification models can reliably determine learning styles, even with minimal labelled data, highlighting the potential of AI-driven personalised learning environments.

Despite the widespread use of learning style questionnaires, traditional self-report methods present several limitations. Bernard et al. (2022) noted that requiring students to complete questionnaires can be time-consuming and may yield inaccurate responses due to self-perception biases. Researchers have proposed automatic methods that analyse students' observed behaviour in digital learning environments to address these challenges. However, no study has comprehensively examined learning styles using diverse student datasets across curricula or disciplines.

Method

This study employed a questionnaire compiled through a comparative analysis of existing questionnaires using machine learning (ML) algorithms to reduce the number of questions while retaining the content of the most meaningful ones.

Questionnaires for Learning Style Definition

Understanding how students learn best is crucial for effective teaching and academic success. Learning styles refer to an individual's preferred way of processing information. Educators often use questionnaires to identify students' learning styles and adapt teaching strategies accordingly. This article examines various questionnaires used to define learning styles, their effectiveness, and the implications of these assessments in educational settings.

One of the most widely used learning style frameworks is the VAK model, which classifies learners into three categories:

● Visual learners prefer images, charts, and written text.
● Auditory learners learn best through listening and discussions.
● Kinesthetic learners tend to retain information more effectively through hands-on experiences.

The VAK Learning Style Questionnaire (Barbe et al., 1979) helps students determine their dominant learning mode by answering preference-based questions.

Kolb's Experiential Learning Theory (ELT) (Kolb, 1984) defines learning as a four-stage process, resulting in four learning styles:

- Accommodating (hands-on, trial-and-error learners)
- Diverging (creative, emotional, and idea-generating learners)
- Assimilating (logical, structured, and theory-based learners)
- Converging (problem-solving, technical, and practical learners)

The Kolb Learning Style Inventory (LSI) is a self-assessment tool that identifies how individuals prefer to learn based on their experiences.

Expanding on VAK, Fleming (2001) introduced the VARK model, which includes:

- Visual (V): Graphs, charts, diagrams.
- Auditory (A): Discussions, lectures, podcasts.
- Reading/Writing (R): Notes, textbooks, written explanations.
- Kinesthetic (K): Hands-on practice, real-life examples.

The VARK Questionnaire is commonly used in schools and universities to tailor study techniques to students' learning styles.

Gardner's Multiple Intelligences Theory (Gardner, 1983) proposes that individuals learn differently beyond traditional styles. The Multiple Intelligences Questionnaire assesses strengths in:

- Linguistic
- Logical-mathematical
- Spatial
- Musical
- Bodily-kinesthetic
- Interpersonal
- Intrapersonal
- Naturalistic

This framework is widely used in personalised education to create diverse learning experiences.

Research on learning styles remains controversial. While some studies support the use of this approach in enhancing student engagement (Pashler et al., 2008), others argue that adapting teaching to specific learning styles does not significantly improve performance (Coffield et al., 2004). Critics suggest a flexible and multimodal approach is more effective than rigid learning style categorisations.

Since no study has employed dynamic tracking of student learning style changes, this study's novelty lies in developing a method for tracking the dynamics of learning style changes and measuring the impact of changing

learning styles on student learning success.

Optimal Number and Content of Questions to Assess a Student's Learning Style

The goal is to balance accuracy and efficiency, providing enough questions to reliably assess a student's style without becoming boring or tedious.

Standard models and recommended number of questions:

- The official VARK questionnaire, developed by Fleming (2001), consists of 16 questions. A shorter version with 8–10 questions is available, but it may reduce accuracy.
- The optimal number of questions in the Kolb Learning Styles Questionnaire (Kolb, 1984) is 12–16, with extended versions including up to 20 questions for greater accuracy.
- The Honey and Mumford questionnaire (1986) contains 80 questions, but research suggests that 40–50 questions are often sufficient for reliable results.
- The number of questions in the Multiple Intelligences Questionnaire (Gardner, 1983) is 30–50, and some versions contain 40–50 questions covering several areas of intelligence.

Since the purpose of this study is to repeatedly use the questionnaire to determine a student's learning style, it is advisable to reduce the number of questions to assess learning style without compromising reliability or the quality of the questions. The methodology includes compiling a questionnaire with a minimum number of questions to determine students' primary learning styles, analysing the answers obtained during the learning process to study changes in learning style, and verifying the reliability of the results obtained.

A machine learning algorithm was used to generate robust questions. Questions with a consistent focus, eliminating contradictions and without confusion between visual, auditory, reading-writing and kinesthetic learning, with clear and specific wording that ensures that participants interpret the questions in the same way and cover different aspects of visual learning - comprehension, organisation, and memory (see Figure 1).

Experiment

The developed questionnaire, used on the poll-mill survey platform, was employed within the Erasmus short-term mobility study project framework from March to April 2025, involving 23 students from universities in Germany, Latvia, Lithuania, and Estonia. Students studied four programs for modelling three-dimensional objects. They completed practical tasks in groups of three to four people on making a furnished living room for a student. Learning style questionnaires were administered before and after the students received training. The questionnaires' data were processed, cleaned, coded and combined into a general table of the results obtained (see Figure 1).

student	time	You work best			You retain better					Do you prefer to					Please indicate your preferences when using the educational material in order of importance (1 is low, 5 is high)				
		in group	alone	so – so	seeing visuals or with flashcards	after hearing it spoken	during writing or taking notes while learning	applying it practically	discussing or teaching it to others	talk	listen	read	watch	do and try	video	text files	interactive exercises	tests	pictures
s1	before			1				1	1	1					4	3	5	3	4
	after		1					1						1	5	3	5	3	5
s2	before			1			1	1	1					1	5	2	5	3	4
	after	1			1			1	1					1	5	1	5	3	3
s3	before	1			1		1	1	1					1	4	2	5	3	4
	after			1				1						1	5	1	5	3	3
…	…	…			…					…					…				
s21	before	1			1			1	1	1					3	3	4	2	4
	after	1			1	1		1	1	1					3	4	4	4	5
s22	before			1	1	1	1	1	1	1					3	4	5	1	2
	after			1	1	1	1	1	1				1		4	3	5	1	2
s23	before	1			1	1		1	1	1					3	4	5	1	2
	after			1	1	1					1				5	5	5	5	5

Figure 1. An Example of The Data Obtained from The Questionnaire (Ovtšarenko, 2025: Learning_style_data).

Figure 1 illustrates the processed data from student surveys, comparing the results before and after learning with individual and group tasks. The results of the students' responses without changes in learning style are shown in yellow, and the changes in learning style are shown in green. The results of the calculated data and visualisation using Python algorithms are presented in Figure 2.
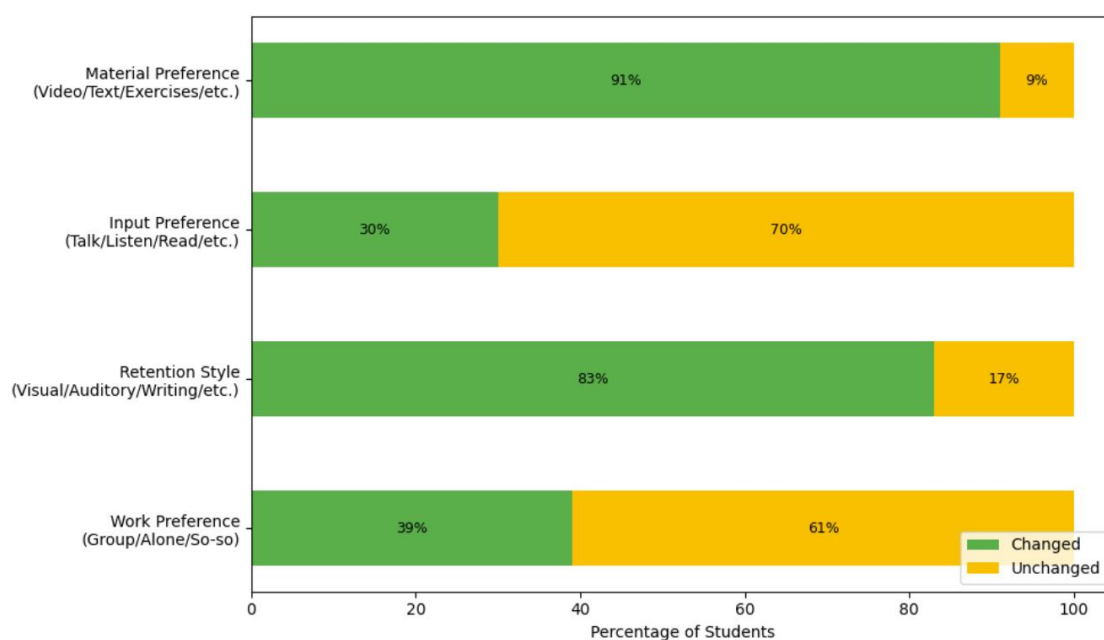

Figure 2. Changes in Students' Learning Styles After the Course.

Results

Analysing the data obtained (see Figure 2):

● Work Preference (Group/Alone/So-So) – 39.1%. This means that 39.1% of the participants showed a clear and consistent preference regarding their work style – whether they prefer to work in a group, individually, or neutral (So-So). The majority (approximately 60.9%) exhibited various responses, showed no clear preference, or were inconsistent in their responses to the work styles.

● Remembering Style (Visual/Auditory/Written/Etc.) – 83%. Here, 83% of the participants demonstrated a clear and consistent preference for a specific method of information retention, such as visual, auditory, or written learning. This high percentage indicates a reliable and consistent tendency among the students regarding how they best remember information. That is, remembering style is a relatively stable and distinguishable trait among the participants.

● Input Preference (Speaking/Listening/Reading, etc.) - 30%. Only 30% of participants clearly preferred their input method (e.g. speaking, listening, reading). This means that most participants either lack a fixed procedure for processing incoming information or their preferences vary depending on the context or task type.

● Material Preference (Video/Text/Exercises, etc.) - 91%. The highest percentage, 91%, indicates that almost all participants strongly preferred certain learning materials (e.g., videos, text resources, or exercises). This extremely high consistency suggests that material preference is the most definable and easily measurable characteristic of learning style among the studied individuals.

Interpretation

Material preference (91%) and retention style (83%) are highly stable and can be effectively used for personalised learning strategies. Work preference (39.1%) and input preference (30%) show much lower stability, suggesting that students may adapt their preferences depending on their circumstances or that these dimensions are inherently more flexible.

Thus, when developing optimised learning style assessments or personalised educational interventions, more attention should be paid to retention style and material preference, as these categories are more reliably determined based on student responses.

Discussion and Limitations

The reliability of the findings can be assessed by examining the consistency of participants' responses across the

different learning style dimensions. The results show that specific categories, particularly Material Preference (91%) and Learning Style (83%), exhibit high internal consistency. Such high percentages suggest that these aspects of learning style are stable and widely represented in individual learners' profiles. Therefore, data from these categories may be reliable for informing personalised instructional strategies.

In contrast, Work Preference (39.1%) and Input Preference (30%) showed significantly lower levels of consistency. These results suggest that learners prefer working alone or in groups, and their preferred input modes (speaking, listening, or reading) are more situational or less developed. Therefore, recommendations based on these dimensions should not be made, given that these preferences may fluctuate depending on the task, context, or mood.

Given the robustness demonstrated in the Material Preference and Learning Style categories, there is a strong basis for using these data to develop practical, personalised instructional recommendations. Instructors can confidently tailor learning experiences by offering students materials and activities that align with their preferred retention methods (e.g., visual aids, written exercises, audio materials) and content formats (e.g., videos, textbooks, interactive exercises). Personalising instruction based on these stable preferences can improve engagement, motivation, and academic achievement.

The results support the need for further use of learning style questionnaires. Shortened and optimised questionnaires that focus on reliable measurement will reduce student fatigue while maintaining the quality of the information obtained. Such questionnaires can be effectively integrated into instructional practices without overwhelming students or instructors.

While the results of this study offer valuable information about the robustness of learning style assessments, several limitations should be acknowledged. First, the study relied on self-reported data, possibly subject to self-perception bias. Second, administering a survey to a relatively small group may limit the generalizability of the results to larger, more diverse groups of students. Additionally, this assessment does not account for potential changes in learning preferences over time or across different stages of schooling. Future research should validate optimised surveys with multiple groups, tracking stability/change in learning styles over time, and examine the impact of personalised educational interventions based on survey data.

Conclusion

This study examined the reliability of data obtained from learning style assessments across four key dimensions: Work Preference, Retention Style, Input Preference, and Material Preference. The results reveal a clear differentiation in the stability and consistency of responses across these dimensions. Material Preference and Retention Style exhibited particularly high levels of reliability (91% and 83%, respectively), indicating that students demonstrate strong and stable preferences in the types of materials they engage with and the methods

they use to retain information. In contrast, Work Preference and Input Preference showed considerably lower consistency (39.1% and 30%, respectively), suggesting that preferences in these areas are either less fixed or more contextually dependent.

These findings have significant implications for personalising learning. Reliable dimensions such as Material Preference and Retention Style can be robust foundations for developing tailored educational recommendations. Educators can potentially enhance engagement, motivation, and academic achievement by aligning instructional methods and learning resources with students' stable preferences. Conversely, dimensions showing lower reliability should be interpreted with greater flexibility. Rather than forming the primary basis for personalisation, Work and Input Preferences may be better understood as situational tendencies that evolve over time and with experience.

The results underline the potential value of using optimised questionnaires for learning style assessment. Streamlining the number of questions, focusing on the most reliable dimensions, and periodically re-evaluating students' preferences could significantly enhance the practicality of these assessments within everyday educational settings. Such optimisation would reduce the time and cognitive load required from students and maintain high standards of reliability and validity in the data collected.

Recognising the dynamic nature of learning styles and the influence of external factors such as subject matter, teaching context, and personal development is essential. Therefore, while learning style data can meaningfully inform personalised learning strategies, it should not be used in a rigid or prescriptive manner. Instead, it should complement broader pedagogical frameworks prioritising flexibility, ongoing assessment, and responsiveness to students' changing needs.

Recommendations

Questionnaires play a valuable role in identifying students' learning preferences, but they should be used in conjunction with dynamic teaching strategies rather than as strict labels. A blended approach incorporating multiple learning methods is recommended to achieve the best educational outcomes.

Using learning style strengths improves:

● Knowing your learning style can help you retain information more effectively.
● Mixing learning styles will help speed up the pace of learning:
● Different note-taking methods, retelling information, and using pictures or diagrams to aid in information processing are all helpful. Using alternative or combined methods is beneficial.
● Knowing your strengths and adjusting your learning method can increase your learning productivity. Focusing on each topic allows you to absorb more information in less time.

● A sense of accomplishment from learning new skills or information leads to confidence, faster and more effective learning, and expanding the student's knowledge base.

References

Al Qahtani N., Al Moammar K, Taher S, AlBarakati S, Al Kofide E. (2018). Learning preferences among dental students using the VARK questionnaire: A comparison between different academic levels and gender. *J Pak Med Assoc*., 68(1):59–64.

Altamimi, A. M., Azzeh, M., and Albashayreh, M. (2022). Predicting students' learning styles using regression techniques.

Ayyoub, H. Y. and Al-Kadi, O. S. (2024). Learning Style Identification Using Semisupervised Self-Taught Labeling, *IEEE Transactions on Learning Technologies*, vol. 17, pp. 1093-1106. doi: 10.1109/TLT.2024.3358864.

Barbe, W., Swassing, R., & Milone, M. (1979). Teaching through modality strengths: Concepts and practices.

Bernard J., E. Popescu, S. Graf (2022). Improving online education through automatic learning style identification using a multi-step architecture with ant colony system and artificial neural networks, *Applied Soft Computing*, Volume 131, 2022, 109779. https://doi.org/10.1016/j.asoc.2022.109779.

Brace, I. (2018) – Questionnaire Design: How to Plan, Structure, and Write Survey Material for Effective Market Research.

Coffield, F., Moseley, D., Hall, E., & Ecclestone, K. (2004). Learning styles and pedagogy in post-16 learning: A systematic and critical review. *Learning and Skills Research Centre.*

De Bruin, G. P., & De Bruin, K. (2011) – Short vs. Long Questionnaires in Psychological Research.

Farkas GJ, Mazurek E, Marone JR. (2026). Learning style versus time spent studying and career choice: Which is associated with success in a combined undergraduate Anatomy and Physiology course? *Anat Sci Educ.*, 9(2):121–3.

Fleming, N. D. (2001). Teaching and Learning Styles: VARK Strategies.

Fleming, N. D. and Mills, C. E. (1992). Not Another Inventory, Rather a Catalyst for Reflection, To Improve the Academy, Vol. 11, p. 137.

Gardner, H. (1983). Frames of Mind: The Theory of Multiple Intelligences. Basic Books.

Honey, P., & Mumford, A. (1986) – The Manual of Learning Styles.

Kolb, D. A. (1984). Experiential Learning: Experience as the Source of Learning and Development. Prentice Hall.

Kurian N, Gowda N R V. (2023). Assessment of learning styles using VARK model in first-year undergraduate medical students. *Indian J Clin Anat Physiol.* 2023;10(3):168-172.

Lincă, F.I. & Matei, F.L. (2024). Learning Styles and Academic Performance Among Students. *Land Forces Academy Review*, Sciendo, vol. 29 no. 1, pp. 63-68. https://doi.org/10.2478/raft-2024-0006.

Ovtsarenko, Olga (2025). Learning_style. *figshare*. Dataset. https://doi.org/10.6084/m9.figshare.28818401.v1.

Pashler, H., McDaniel, M., Rohrer, D., & Bjork, R. (2008). Learning styles: Concepts and evidence.

Psychological Science in the Public Interest, 9(3), 105-119.

Sulistyanto H., J. Nurkamto, M. Akhyar, Asrowi (2019). A review of determining the learning style preferences by using computer-based questionnaires on undergraduate students. J. Phys.: Conf. Ser.. 1175 012209. DOI 10.1088/1742-6596/1175/1/012209.